Reviews

Reduced Molybdenum Phosphates: Octahedral–Tetrahedral Framework Solids with Tunnels, Cages, and Micropores†

Robert C. Haushalter*,[1] and Linda A. Mundi[2]

Exxon Research and Engineering Co., Annandale, New Jersey 08801

Received September 17, 1991. Revised Manuscript Received November 25, 1991

The exquisite shape-selective absorptivities of the zeolites have inspired areas of research ranging from topological theories for filling space to novel hydrothermal experimental techniques to important petrochemical processes. However, the closed shell nature of these silicoaluminates renders them ineffective for many of the types of reactions that the d-block elements are capable of such as atom abstractions and redox chemistries. If one could prepare a heat-stable oxide with shape-selective access to large internal micropore volumes combined with the reactivity of a transition element, then the possibilities of observing new types of shape-selective catalysis could be enhanced. The molybdenum phosphates (MoPO) discussed here represent the beginning steps toward materials of this type. These MoPO's are synthesized hydrothermally in aqueous H_3PO_4 in the presence of a cationic template and contain anionic octahedral–tetrahedral frameworks with the Mo in an oxidation state of ≤5+. Almost all contain Mo–Mo bonds. The discussion will focus mainly on the synthesis, structures, and properties of molecular, large ionic aggregates, one-dimensional polymeric and two-dimensional layered MoPO's culminating in three-dimensional microporous solids, some of which contain nearly 40 vol % accessible internal void space.

1. Introduction

A wide variety of approaches have been developed in attempts to increase the selectivity of chemical reactions. In addition to the manipulation of physical variables such as time, temperature, pressure, etc., scientists have made steady progress toward increasing selectivity by controlling the type and geometric location of the atoms in the immediate environment of a reactive site. While enzymes provide the best examples of selectivity modification by control of the local geometry, synthetic efforts have begun to yield structures with a certain degree of structural order near the active site. Constraints like these have been observed in many different disciplines, such as organic and bioinorganic chemistry, where selectivity can be enhanced by the nature of the proximate organic ligands, as well as in heterogeneous catalysis, where greatly differing reactivities are observed as a function of which crystal planes are exposed. Striking examples are found in the strong size and shape selectivities inherent in many of the zeolitic solids,[3-7] such as silicoaluminates and aluminophosphates. Much work directed toward selectivity has also recently focused on the compartmentalization of chemical reactions, in order to alter normal equilibria, by the incorporation of membrane geometries.

We have recently begun to investigate the preparation of a class of materials in which it may eventually prove possible to incorporate several of these desirable features into one solid-state material. We speculated that a material that would combine a "monodisperse" pore size distribution in the regime of molecular-sized holes to provide the shape selectivity of a zeolite, the thermal and chemical stability of a metal oxide with the reactive sites of a homogeneous or heterogeneous catalyst could provide a totally inorganic pathway to achieve a high degree of chemical selectivity. Qualitatively, one could think of a material of this type as embodying the attributes of a "solid-state inorganic enzyme".

How would one decide which actual system to investigate and what synthetic methods would be required to produce materials of this type? The following points are necessary or desirable: (a) The solid is crystalline: this is needed to achieve the highest degree of absorption specificity; amorphous solids often have a wide pore-size distribution as well as sometimes suffering from a thermodynamic instability with respect to crystalline solids. (b) The pore structure has a high dimensionality, a high degree of connectivity, and a low defect level: an interconnected, 3-D array of pores is less likely to fail to sorb guests due to framework or sorbate decomposition. (c) The synthesis will be carried out at as low a temperature as possible: in general, in analogy with conventional mineralogical wisdom, lower temperatures and pressures favor more open structures. (d) A reasonable degree of chemical and thermal stability is required. (e) The catalytically active site must physically communicate with the pore structure. (f) It should be possible to generate a vacant coordination site on the active transition-metal site. (g) When the templating entity used to form the pore structure is removed, the tunnels must be large enough to absorb the species of interest.

† Dedicated to Prof. Dr. H. G. von Schnering on the occasion of his 60th birthday.

(1) Author to whom correspondence should be addressed. Present address: NEC Research Institute, 4 Independence Way, Princeton, NJ 08540.

(2) Present address: NEC Research Institute, 4 Independence Way, Princeton, NJ 08540.

(3) Barrer, R. M. *Hydrothermal Chemistry of Zeolites*; Academic Press: New York, 1982.

(4) Breck, D. W. *Zeolite Molecular Sieves*; Krieger: Malabar, FL, 1974.

(5) Szostak, R. *Molecular Sieves Principles of Synthesis and Identification*; Van Nostrand Reinhold: New York, 1989.

(6) Occelli, M. L.; Robson, H. E. *Zeolite Synthesis*; American Chemical Society: Washington, DC, 1989.

(7) Meier, W. M.; Olson, D. H. *Atlas of Zeolite Structure Types*; Butterworths: London, 1987.

0897-4756/92/2804-0031$03.00/0

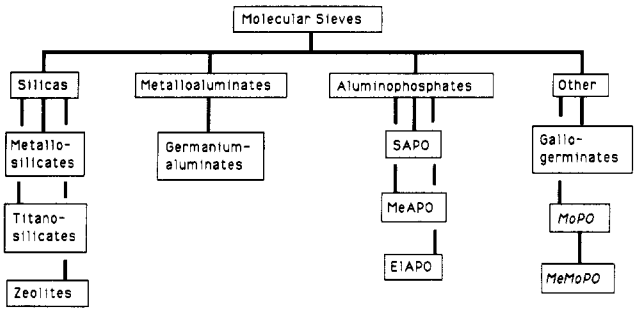

Figure 1. Types of microporous solid (after Szostak[5]). Most known examples are zeolites and AlPO materials.

The attempt to combine many of these features into a solid-state material suggests the following items will have to be considered: (a) A transition element is a vital framework constituent. Chemistry involving oxidation/reduction, free-radical chemistry, photochemical reactions, and atom abstraction reactions is generally facilitated by transition elements. Furthermore, many transition elements are octahedrally coordinated, and it is easier to generate a vacant coordination site on an octahedrally coordinated element, as compared to one with tetrahedral coordination, based on simple electrostatic considerations. (b) Incorporation of silicates and phosphates often impart a high degree of mechanical, chemical, and thermal stability (as in the case of silicate minerals and bones). (c) The relatively high negative charge in SiO_4^{4-} and PO_4^{3-} tetrahedra favors the formation of anionic frameworks. This is important since almost all microporous solids are formed from the removal of a cation from an anionic framework (mainly because many removable templates are large organic cations). (d) The examples provided by most syntheses of zeolites and open mineralogical frameworks suggests that hydrothermal syntheses[8] are most likely to produce open frameworks. (e) When many transition elements, particularly the earlier ones, are considered, formation of M–O–M or M–O–X bonds, which is necessary to assemble the 3-D framework, is favored at low pH and conversely these bonds often undergo hydrolysis at higher pH. Since SiO_2 is not particularly soluble at moderately low pH (as compared to very strong base), combination of (c) and (e) suggests the use of H_3PO_4 both as a phosphate source and an acid.

Therefore the combination of all of the above factors suggests that the hydrothermal synthesis of an anionic, cation occluding, octahedral–tetrahedral framework of a transition-metal phosphate might yield the desired solid-state materials.

2. Related Systems

Only crystalline oxide materials are considered here so amorphous or partially crystalline materials such as amorphous silicas and aluminas, pillared clays, porous carbons, membranes and organic systems are not covered. Also, materials that have been reported without either structure determination or demonstrated absorption into micropores are likewise excluded.

The term "molecular sieve" was first used by McBain in 1932[9] and is applicable in a general sense to solids with internal pore structures capable of sorbing small molecules. A useful broad classification of crystalline, oxide molecular sieves (after Szostak[10]) is shown in Figure 1. The zeolites and aluminophosphate materials account for the bulk of the known microporous solids. The zeolites, of which there are many naturally occurring[11] and synthetic examples, are the best known and most studied type of microporous solid.[3-7] They are composed of anionic silicoaluminate frameworks that contain occluded cations, and usually solvent, within the micropores when initially synthesized. They usually conform to the general formula $M_{x/n}[(AlO_2)_x(SiO_2)_y]\cdot wH_2O$, where x is the valence of the cation and w is the number of water molecules. The ratio of y/x is generally in the range 1–5 (but can be larger) depending on the structure. Note that the substitution of an Al^{3+} for a Si^{4+} generates a negative charge on the framework which is charge compensated by the cation within the micropore. These materials are generally rendered microporous by combustion or thermal removal of the templating organic cations, or in the case of inorganic templates by dehydration or ion exchange. Although it is often easy to ion exchange many types of metal cation into the pores of the zeolites, it is difficult to incorporate large, stoichiometric amounts of metal cations into the framework in an ordered manner.[12] When one is able to incorporate a transition element (e.g., Fe or Ti) into the framework it often substitutes into a tetrahedral site in an apparently random fashion while maintaining the original structure of the zeolite framework.[13]

Another very large class of microporous materials, the aluminophosphates (AlPO), has been developed due to the pioneering work of Flanigen and co-workers.[14] This is a vast field which now contains, with all the framework substitutional variants, more species than the zeolites. Unlike the aluminosilicates, which have a negatively charged framework, the aluminophosphates are inherently neutral, have an invariant Al/P ratio of 1, and contain no Al–O–Al or P–O–P bonds. The framework neutrality results in the incorporation of salts (e.g., tetraalkylammonium hydroxides) instead of cations as in the zeolite frameworks. The aluminum in aluminophosphates is not confined solely to tetrahedral coordination.

Other classes of porous tetrahedral framework solids related to the AlPO phases are the metalloaluminophosphates (MeAPO).[14] This class of materials includes, in addition to the MeAPO (Me = Co, Fe, Zn, Mg, Mn, etc.) solids, the silicoaluminophosphates (SAPO) and quaternary systems containing metals, Si, P, and Al in an oxide matrix.[13] Most of these tetrahedral solids are less acidic than aluminosilicates and therefore are catalytically less reactive in a wide variety of reactions. In addition to the substitutions into zeolite structure types discussed above, other tetrahedral framework solids include phases in the Ge–Al–O and Ga–Ge–O systems, and most are isostructural with known zeolites or minerals.[13]

The non-tetrahedral framework materials that have large pores have mainly octahedral–tetrahedral frameworks, but a few examples of tunnel structures in all octahedral framework materials are known in the systems structurally related to hollandite such as psilomelane, todorokite, etc.[15]

Very recently a new class of microporous materials based on the titanium silicate system has been disclosed in the patent literature.[16] These solids, built up from octahedral

(8) Rabenau, A. *Angew. Chem., Int. Ed. Engl.* **1985**, *24*, 1026.
(9) McBain, J. W. *The Sorption of Gases and Vapors by Solids*; Rutledge and Sons: London, 1932.
(10) Reference 5, p 2.
(11) Reference 5, p 358: A table listing properties and references for 32 naturally occurring zeolites.
(12) Reference 6, Chapters 23, 25–29.
(13) Reference 5, Chapter 4.
(14) Reference 6, Chapter 23; ref 5, Chapter 4.
(15) Vaughan, D. E. W. In *ZEOLITES: Facts, Figures, Future*; Jacobs, P. A.; van Santen, R. A., Eds.; Elsevier: New York, 1989; pp 95–116.
(16) U.S. Patent 4,853,202; European Patent Appl. 0405978 A1.

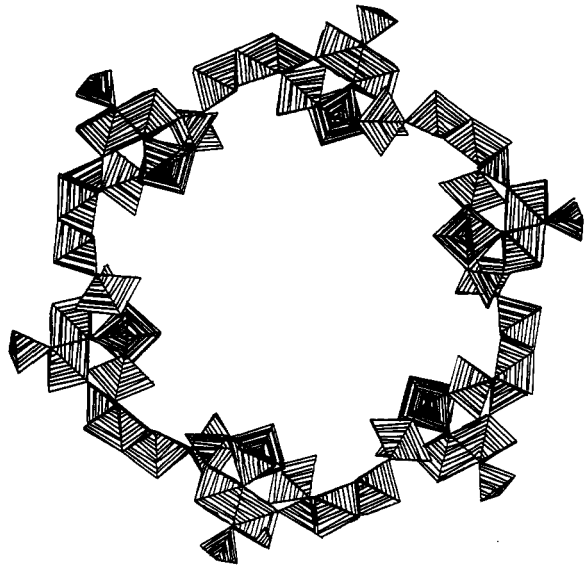

Figure 2. Portion of the structure of cacoxenite showing the giant 14.2-Å diameter tunnel which is filled mainly with water.

titanium and tetrahedral silicon components, appear to be one of the few bona fide examples of a synthetic microporous octahedral–tetrahedral framework solid. They were discovered by Kuznicki and co-workers at Englehard and are referred to as ETS (Englehard titanium silicates). The sorption data reported leave no doubt that they have open pores that are large enough, at least in certain of the materials, to sorb appreciable amounts of even branchy hydrocarbons. Some other Ti–Si–O frameworks were also recently reported by Chapman and Roe.[17]

There are, however, some amazing mineral structures with open octahedral–tetrahedral frameworks that were formed in hydrothermal environments. The most famous example is Moore's determination of the structure of the phosphate cacoxenite,[18] $AlFe_{24}O_6(OH)_{12}(PO_4)_{17}(H_2O)_{17}\cdot 51H_2O$, which contains the largest pores ever observed in a solid at 14.2 Å. The structure is shown in Figure 2. Another exceedingly complex octahedral–tetrahedral framework is found in the structure of betpaktalite,[19] a portion of which is shown in Figure 3. Although the structure was reported several years ago, it was not until a critical examination of the structure by Moore[20] did it become apparent that the structure is incredibly open. The oxygen atoms occupy only 46% of the available volume! In spite of this amount of vacancies, the remaining oxygens are still nearly *exactly* at the positions predicted from the closest packing of spheres. The structures of cacoxenite and betpaktalite illustrate several very important points: (a) We know essentially nothing about the factors affecting hydrothermal syntheses or the correlations of the structure obtained with the reaction conditions. Although most of the syntheses are perfectly reproducible, it is essentially impossible to plan the syntheses of radically new materials. (b) Amazingly complex structures can be produced rivaling the most complicated organic systems. (c) It is very difficult to visualize and comprehend the structures even if the crystal structures are known. This latter point was addressed recently by Moore, who observed[20] "with the advent of canned programs competency

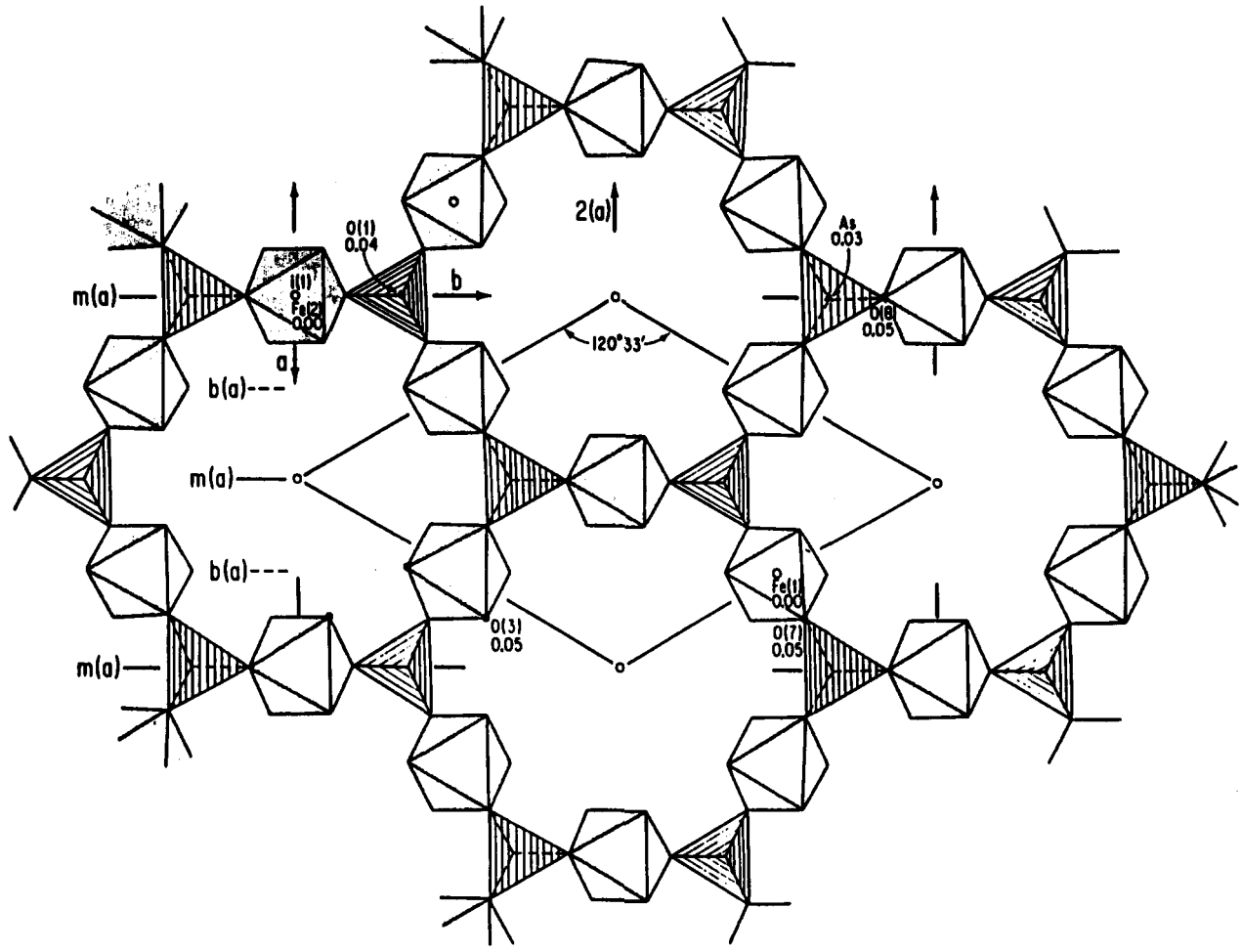

Figure 3. Slice through the betpaktalite structure showing the large voids (picture courtesy of Paul Moore).

of structure display has noticeably deteriorated [and] if misrepresented, the structures can 'slip into the grey gloom, an abandoned orphan of science'." We have tried to address this problem here by the use of depth-queued color figures for the more complicated structures. But this is a poor substitute for holding a model in your hands for visual inspection. One should not be daunted, however, as these difficulties strongly signal that this is an area ripe for much further research!

The remainder of this review will discuss the synthesis, structure, and properties of the octahedral–tetrahedral frameworks found in the reduced molybdenum phosphate system. There are scattered examples in the literature of molybdenum silicophosphates[21] and other miscellaneous molybdenum phases that will not be discussed here.

3. Reduced Molybdenum Phosphates

The materials discussed here are all built up from MoO_6 octahedra and PO_4 tetrahedra. Only molybdenum in oxidation states less than 6+ are considered. A large class of molybdenum phosphates not discussed here, the so-called Keggin ions and related species[22] which display Mo:P ratios of 12:1, have average oxidations states of greater than 5+.

Molybdenum is well-known for its ability to assume many different oxidation states. Many of the MoPO materials discussed below have Mo in the 5+ oxidation state with a d^1 configuration. When in the 5+ oxidation state, molybdenum very often displays a coordination geometry where the Mo is well off center in its (usually quite regular) octahedron of O atoms[23] due to the formation of the O—Mo=O unit with a short Mo=O bond (near 1.6 Å) trans to a much longer Mo—O (near 2.3 Å). Another characteristic of Mo^{5+} is its tendency to form dimers with Mo—Mo single bonds near 2.6 Å which results in the pairing of the two d electrons. This edge sharing octahedral coordination is illustrated in 3-1 and many of the MoPO's discussed below share this feature.

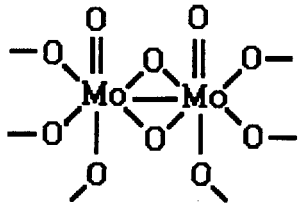

3-1

The other oxidation states of Mo (3 to <5+) found in the molybdenum phosphates generally have more regular octahedral coordination. The polyhedral vertex connectivity mode found most often in the MoPO materials is that of corner sharing. The PO_4 tetrahedra only share their corners, while the MoO_6 octahedra share corners predominantly but also occasionally share their edges and faces as well.

Many of the hydrothermally prepared Mo^{5+} materials discussed below, which have both organic cations as well as hydronium or metal cations as the pore filling entities, display a common structural element. This element is the proximity of the relatively less polar molybdenyl groups to the nonpolar alkylammonium cations while the polar inorganic cations associate with the P–O and P–O–H groups. This effect will be discussed for applicable individual compounds below.

Several of the primary building blocks that have been observed in the MoPO's thus far are shown in Figure 4 and will be covered in detail when the compounds in which they are found are discussed. The discussion of the phosphates below will be organized according to the basis of connectivity: a few examples each of molecules and ionic aggregates, one-dimensional (1-D) polymers, 2-D layered materials will be given with the most emphasis placed on solids possessing covalent bonds in three dimensions.

Many of the compounds discussed in this article are collected in Table I.

1. Molecules and Ionic Aggregates. Strictly molecular, mononuclear metal complexes with phosphate ligands that do not contain hydrogen bonds or ionic bridges to their neighbors are very rare because it is geometrically impossible for all of the O atoms of a PO_4 group to bond to one metal center. One of the first examples of a reduced MoPO, which contains Mo–Mo triple bonds, was found in $Cs_2[Mo_2(HPO_4)_4(H_2O)_2]$,[24] which contains molecular $Mo_2(HPO_4)_4^{2-}$ units H-bonded into a 3-D array.

In our hydrothermal syntheses of MoPO's we have found multinuclear Mo clusters ranging from around 30 to over 250 atoms (including the oxo ligands), several of which are based on the $Mo_6O_{15}(HPO_4)(H_2PO_4)_3^{5-}$ building unit which is shown in Figure 4a. There are two important features to note about this anion: (a) it has been found in all structures to date as a dimer with two of the $Mo_6O_{15}(HPO_4)(H_2PO_4)_3^{5-}$ units bonded together by either an alkali or transition metal to give $\{M^{n+}[Mo_6O_{15}(HPO_4)(H_2PO_4)_3]_2^{(10+n)-}\}$ (1) clusters. Note that the central metal M is octahedrally coordinated by three O atoms from each Mo_6P_4 ring, thus making the Mo–Mo bonds and the pendant PO_4 groups on the two rings staggered relative to each other, and is shielded from the external environment by the twelve interpenetrating molybdenyl groups (Figures 4a and 5). Also it can be seen that the oxide ions in 1 form a nearly close-packed array with the cations in between the layers and (b) in most cases where the crystal structure contains both nonpolar (e.g., tetraalkylammonium) and polar (e.g., Na^+, NH_4^+, H_3O^+) cations, the Mo=O groups are associated with the nonpolar cations and the phosphate P—O groups, on the "ends" of the dimer, are associated with the polar cations. Thus 1 appears to be amphiphilic and the crystal packing in several MoPO solids can be rationalized on the basis of these hydrophobic–hydrophilic interactions.

An illustration of this phenomenon is found in the ionic aggregate $(Et_4N)_6Na_2[Na_{12}(H_3PO_4)\{Mo_6O_{15}(HPO_4)(H_2PO_4)_3\}_4]\cdot xH_2O$,[25] 2 (Figure 7). The large $[Na_{12}(H_3PO_4)\{Mo_6O_{15}(HPO_4)(H_2PO_4)_3\}_4]^{8-}$ cluster (Figure 6) contains a central H_3PO_4 tetrahedron encapsulated within a distorted icosahedron of Na^+ (Figure 8) which are bound to the 16 PO_4 groups of the four $Mo_6O_{15}(HPO_4)(H_2PO_4)_3$ units (Figure 4a). This entire aggregate, which has site symmetry 23 in $Pn3$, is bound to identical aggregates via Na^+ cations, which generates a 3-D array

(17) Chapman, D. M.; Roe, A. L. *Zeolites* **1990**, *10*, 730.
(18) Moore, P. B.; Shen, J. *Nature* **1983**, *306*, 356.
(19) Schmetzer, K.; Nuber, B.; Tremmel, G. *Neues Jb. Mineral. Mh.* **1984**, 393.
(20) Moore, P. B. *Aust. J. Chem.*, in press.
(21) Leclaire, A.; Lamire, L.; Raveau, B. *Acta Crystallogr.* **1988**, *C44*, 1181. Leclaire, A.; Monier, J. C.; Raveau, B. *Acta Crystallogr.* **1984**, *B40*, 180. Wang, S. L.; Wang, C. C.; Lii, K. H. *J. Solid State Chem.* **1988**, *74*, 409.
(22) Pope, M. T.; Müller, A. *Angew. Chem., Int. Ed. Engl.* **1991**, *30*, 34.
(23) Cotton, F. A.; Wilkinson, G. *Advanced Inorganic Chemistry*, 5th ed.; New York, 1988; p 824.
(24) Bino, A.; Cotton, F. A. *Angew. Chem., Int. Ed. Engl.* **1979**, *18*, 462.
(25) Haushalter, R. C.; Lai, F. W. *Angew. Chem., Int. Ed. Engl.* **1989**, *28*, 743.

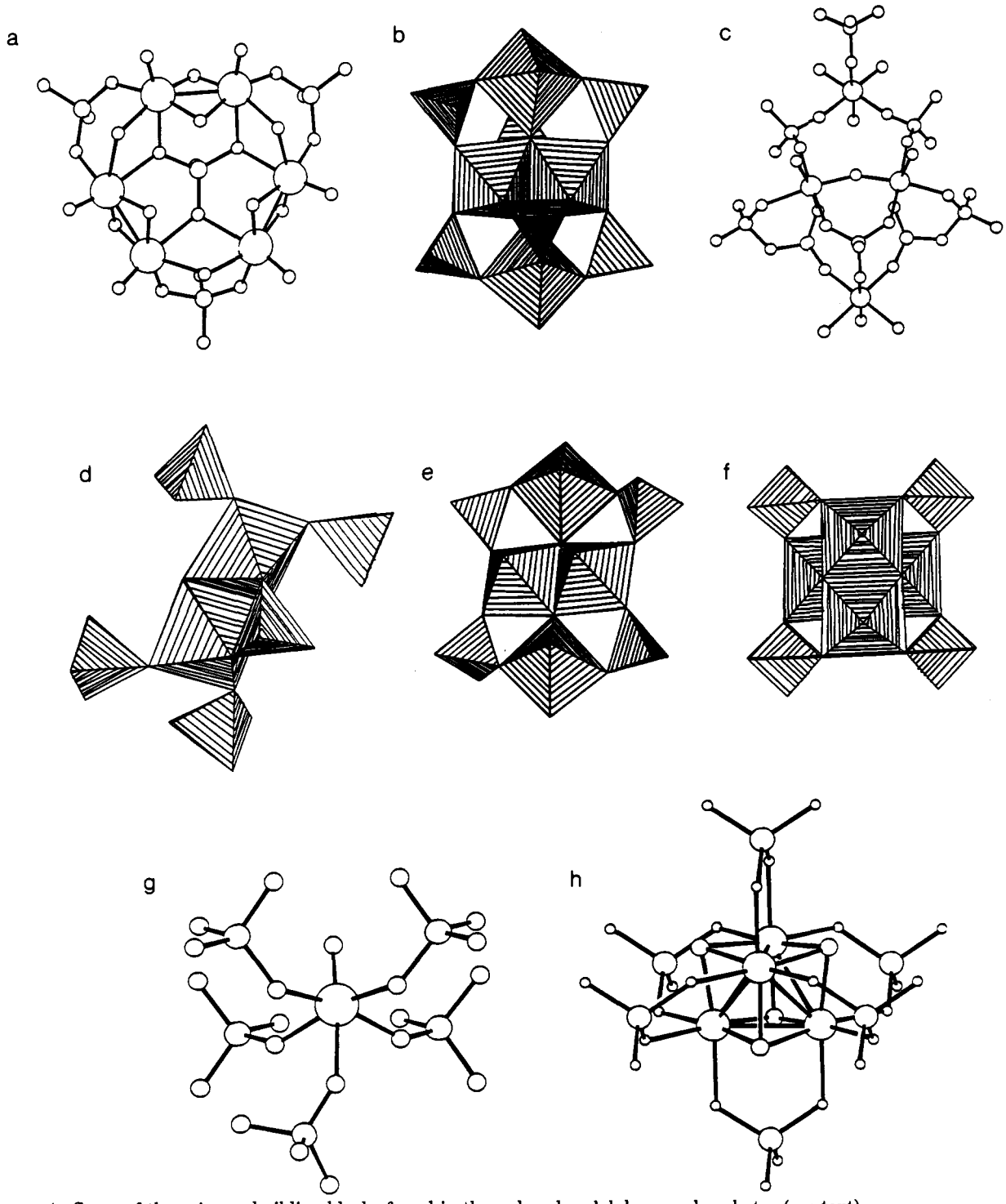

Figure 4. Some of the primary building blocks found in the reduced molybdenum phosphates (see text).

of intersecting tunnels in which the Et_4N^+ cations reside. Thus these $[Na_{12}(H_3PO_4)\{Mo_6O_{15}(HPO_4)(H_2PO_4)_3\}_4]^{6-}$ units are bonded to each other with a symmetry very similar to that of the carbon atoms in diamond. The unit cell contents are shown in Figure 6 which illustrates the hydrophobic–hydrophilic association of the $Na^+/P—O$ and $Mo=O/ET_4N^+$ moieties. Note that the polar material is inside the cluster and the relatively less polar molybdenyl groups are oriented toward the nonpolar Et_4N^+ cations in the tunnels. A somewhat similar aggregate, but with more covalent bonds holding the Mo_6P_4 units together, is found in $[(H_3PO_4)Na_8In_4(H_2O)_4\{Mo_6O_{15}(HPO_4)(H_2PO_4)_3\}_4]$.[26]

The phosphate $(PPh_4)_2[(H_3O)_2NaMo_6O_{15}(HPO_4)(H_2PO_4)_3$[27] contains these same Mo_6P_4 units bridged by sodium cations into 1-D strings that are surrounded by PPh_4^+ cations.

2. One-Dimensional Polymers. Phosphate $(Et_4N)_2[Mo_4O_8)(PO_4)_{2/2}(H_{1.5}PO_4)_2]\cdot 2H_2O$,[28] **3**, is the only 1-D covalently bonded MoPO without transition elements as a part of the repeat unit. This is a very unusual material (Figure 9) in that it is one of the few examples of a 1-D transition oxide polymer. The polymer is built up from

(26) Haushalter, R.; Mundi, L.; unpublished results.

(27) Haushalter, R. C.; Lai, F. W. *Inorg. Chem.* **1989**, *28*, 2904.

(28) Mundi, L.; Strohmaier, K. G.; Goshorn, D. P.; Haushalter, R. C. *J. Am. Chem. Soc.* **1990**, *112*, 8182.

Table I

compound	composition	cell parameters	space group	ref	figure
2	$(Et_4N)_6Na[Na_{12}(H_3PO_4)\{Mo_6O_{15}(HPO_4)(H_2PO_4)_3\}_4]\cdot xH_2O$	a = 20.040 (1) Å	$Pn\bar{3}$	25	6
3	$(Et_4N)_2[Mo_4O_8(PO_4)_{2/2}(H_{1.5}PO_4)_2]\cdot 2H_2O$	a = 12.235 (8) Å b = 19.141 (4) Å c = 7.497 (4) Å	$P2_12_12$	26	9
4	$Cs_2Mo_4P_6O_{26}$	a = 6.398 (1) Å b = 19.497 (6) Å c = 9.835 (2) Å β = 107.06°	$P2_1$	29	11
5	$Na_3[Mo_2O_4(HPO_4)(PO_4)]c2H_2O$	a = 8.128 (3) Å b = 13.230 (4) Å c = 11.441 (2) Å	$P2_1/n$	30	12
6	$Pr_4N(NH_4)[Mo_4O_8(PO_4)_2]$	a = 7.512 Å c = 11.384 Å	$P\bar{4}2m$	32	13a
7	$(Et_2NH_2)_2[Mo_4O_8(PO_4)_2]$	a = 7.5536 (9) Å c = 20.545 (3) Å	$I\bar{4}$	33	13b
8	(4-phenylpyridine)$_2[Mo_4O_8(PO_4)_2]$	a = 14.717 (6) Å b = 7.535 (4) Å c = 26.317 (7) Å β = 105.15°	$P2/c$	33	14
10	$Cs_3Mo_6P_{10}O_{38}$	a = 9.502 (2) Å b = 14.219 (3) Å c = 6.425 (5) Å α = 91.07° β = 106.04° γ = 90.09°	$P\bar{1}$	58	16a
11	$Cs_4Mo_6P_{10}O_{38}$	a = 9.659 (2) Å b = 14.404 (5) Å c = 6.446 (2) Å β = 105.58°	$P2_1/m$	59	16b
12	$Cs_3Mo_4P_3O_{16}$	a = 7.728 (4) Å	$P\bar{4}3m$	61	17
13	$Cs_3Mo_5P_6O_{25}$	a = 11.868 (4) Å c = 9.352 (2) Å	$P31c$	66	
14	$(Me_4N)_{1.3}(H_3O)_{0.7}[Mo_4O_8(PO_4)_2]\cdot 2H_2O$	a = 15.049 (2) Å	$I\bar{4}3m$	67	
15	$Mo_8O_{12}(PO_4)_4(HPO_4)_2\cdot 13H_2O$	a = 10.466 (5) Å b = 12.341 (4) Å c = 8.228 (7) Å α = 94.75° β = 111.46° γ = 89.48°	$P\bar{1}$	68	21
16	$NH_4[Mo_2P_2O_{10}]\cdot H_2O$	a = 9.78 (1) Å b = 9.681 (5) Å c = 9.884 (8) Å β = 102.17°	$P2_1/n$	69	22
17	$H_3O[Mo_2O_2(PO_4)_2(H_2PO_4)]\cdot xH_2O$	a = 6457 (2) Å c = 15.996 (5) Å	$I422$	72	25a
18	$CH_3NH_3[Mo_2O_2(PO_4)_2(H_2PO_4)]$	a = 9.126 (6) Å b = 9.108 (8) Å c = 8.654 (3) Å β = 114.06°	$C2$	73	25b
19	$Cs(H_3O)[Mo_2O_2(PO_4)_2(HPO_4)]$	a = 9.166 (4) Å b = 9.073 (2) Å c = 15.808 (3) Å β = 96.85°	$P2_1/n$	74	25c
20	$(NH_4)_3Mo_4P_3O_{16}$	a = 7.736 (2) Å	$P\bar{4}3m$	75	

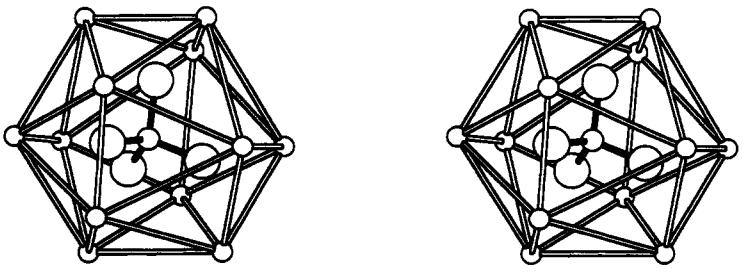

Figure 8. Stereoview of the central phosphate in **2** surrounded by the distorted icosahedron of twelve Na^+ ions. See also Figures 6 and 7.

Mo_4O_8 cubes (Figure 4f), which have approximate point symmetry $\bar{4}2m$, all of the Mo in the 5+ oxidation state and two Mo–Mo bonds near 2.6 Å. These cubes are connected into the 1-D chain by $(PO_4)_{2/2}$ tetrahedra and have two terminal $H_{1.5}PO_4$ groups. The polymer displays an unusual type of chirality and has only one enantiomer present in each crystal. These 1-D chains are hydrogen bonded into sheets (Figure 10), by extremely short H bonds (2.28 (5) Å), that are interleaved by the Et_4N^+ cations.

Two other covalently bonded 1-D MoPO's exist but are metallomolybdenum phosphates with Fe bridging the MoPO moieties together.[26]

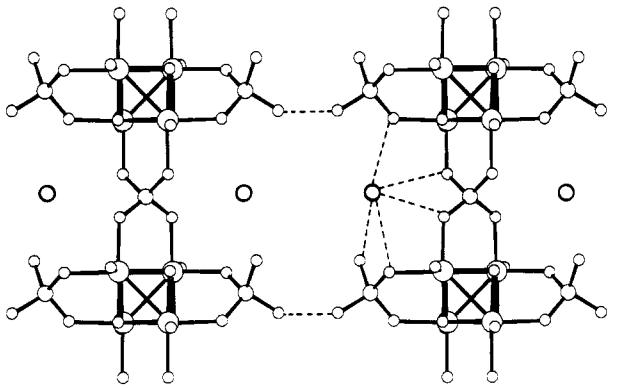

Figure 10. Illustration of how the 1-D chains in $(Et_4N)_2[Mo_4O_8(PO_4)_{2/2}(H_{1.5}PO_4)_2]\cdot 2H_2O$ are hydrogen bonded (dashed lines) into 2-D sheets. These sheets are in turn interleaved with Et_4N^+ groups in the solid.

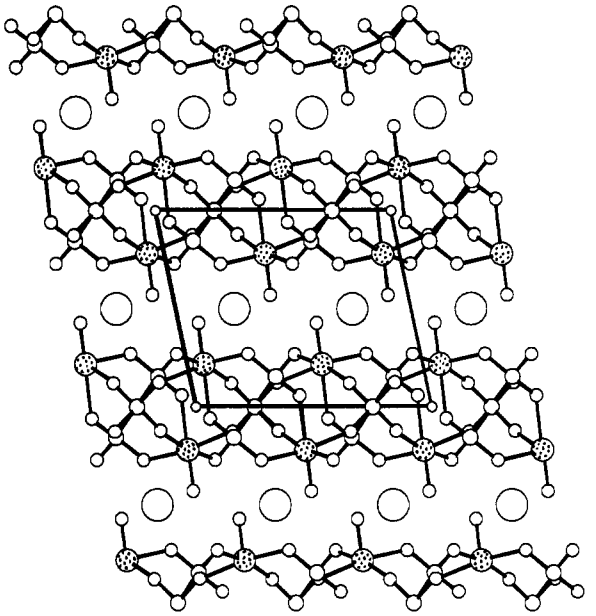

Figure 11. Ball-and-stick representation of the structure of $Cs_2Mo_4P_6O_{26}$. The Mo atoms are stippled, and the large interlamellar circles are Cs^+. View down [010].

3. Two-Dimensional Layered Materials. There are quite a few examples of layered MoPO's, including those synthesized at high temperature and several prepared hydrothermally. The main possibilities for the atom terminating the layers, in the materials prepared at high temperatures, are a M=O (found with Mo^{5+}) or a P—O^- entity because P—O—H groups would be dehydrated at these temperatures.

The compound $Cs_2Mo_4P_6O_{26}$,[29] **4**, which is built up from corner-sharing MoO_6, PO_4, and P_2O_7 polyhedra connected in the sequence ...$(PO_4)(MoO_6)(P_2O_7)(MoO_6)(PO_4)$... and is shown in Figure 11, constitutes the only example of a high-temperature layered MoPO. It has Mo=O groups protruding into the intermellar space. This material was always obtained mixed with another MoPO with exactly the same stoichiometry as **4**, but with a 3-D structure, discussed below. Many of the MoPO's prepared at high temperature such as **4** contain Mo:P ratios <1 which results in the absence of Mo—O—Mo bonds and/or the presence of P_2O_7 groups.

The hydrothermally prepared layered MoPO's are all synthesized at $T \leq 200$ °C and have Mo:P ≥ 1 and, since they are prepared in water, no P_2O_7 groups. The phosphate **5**, $Na_3[Mo_2O_4(HPO_4)(PO_4)]\cdot 2H_2O$,[30] crystallizes in a unique structure type containing edge sharing MoO_6 octahedra with a Mo–Mo bond of 2.575 (2) Å (Figure 12). The dimolybdenum unit in this structure is shown in Figure 4d with its surrounding phosphate groups. One of two crystallographically unique PO_4 groups has an edge that bridges the two vertices of the Mo dimer trans to the molybdenyl group while the other one connects three different Mo_2O_{10} dimers together. Each type of PO_4 group has a terminal P–O bond, but charge balance requires only one H^+ for the two P–O. Thus the structure appeared as if it may support proton, as well as Na^+, ionic conduction, both of which have been borne out by subsequent experiments.[31]

There are several examples of layered MoPO's comprised of $[Mo_4O_8(PO_4)_{4/2}]^{2-}$ building blocks (Figure 4f), all of which are prepared hydrothermally. The motif of these layers is built on that of "cubes" and PO_4 tetrahedra. The cubes are actually composed of four triply edge-sharing octahedra. Two of the six cube faces have the four Mo=O groups and the two Mo—Mo bonds, as in the case of the similar core unit in **1**, with the other four faces coordinated to four $(PO_4)_{2/2}$ groups.

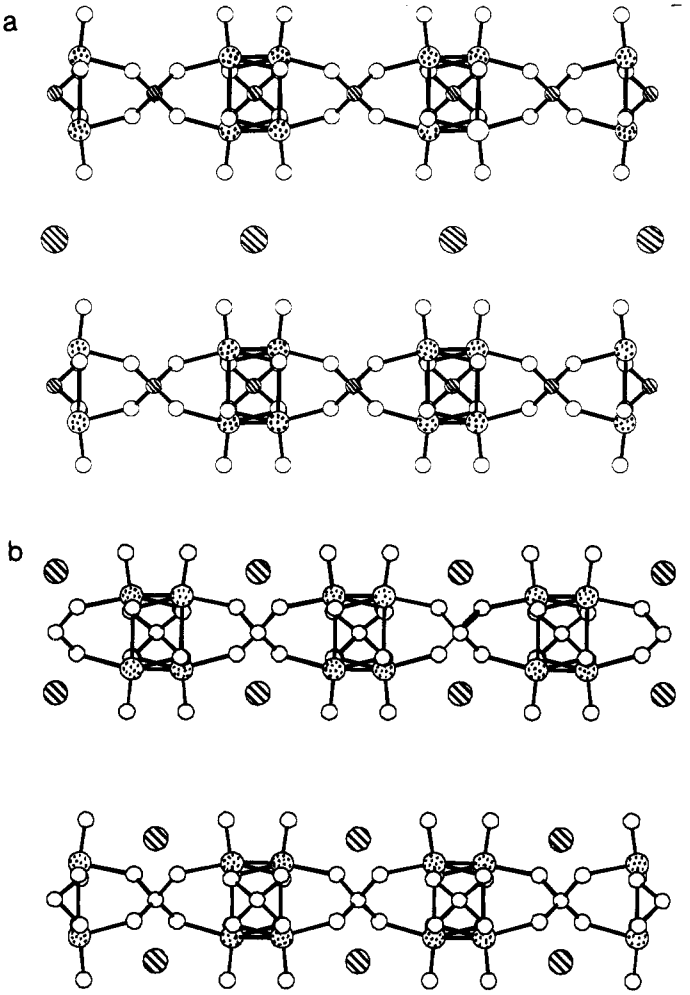

Figure 13. Primitive and body-centered tetragonal stacking sequences for, respectively, the planar $[Mo_4O_8(PO_4)_2]^{2-}$ layers found in (a) $Pr_4N(NH_4)[Mo_4O_8(PO_4)_2]$ ($P\bar{4}2m$) and (b) $(Et_2NH_2)_2[Mo_4O_8(PO_4)_2]$ ($I\bar{4}$). The striped circles represent the N atoms of the tetraalkylammonium groups, and the Mo atoms are stippled.

(29) Lii, K. H.; Haushalter, R. C. *J. Solid State Chem.* **1987**, *69*, 320.

(30) Mundi, L. A.; Haushalter, R. C. *Inorg. Chem.* **1990**, *29*, 2879.

(31) Tsai, M.; Feng, S.; Greenblatt, M.; Haushalter, R. C. *Solid State Ionics*, in press.

Two types of these layers containing these building blocks have been observed: one type that is planar with symmetry $\bar{4}2m$ and one that is puckered. Note that these layers are inherently acentric. Examples of the planar sheets (Figure 13a,b) are found in $Pr_4N(NH_4)[Mo_4O_8(PO_4)_2]$,[32] **6** (*P* centered lattice with one layer per stacking repeat) and $(Et_2NH_2)_2[Mo_4O_8(PO_4)_2]$,[33] **7** (*I* centered with two layers per stacking repeat). The puckered sheet has been found in (4-phenylpyridine)$_2[Mo_4O_8(PO_4)_2]$,[33] **8**, and is shown in Figure 14. Note that in **6**–**8** the N—H bonds (polar heads) are associated with the P—O regions. Also the alkyl groups are near the Mo=O moieties. The severe ruffling of the layers in **7** is most likely due to the stacking of the cations to maximize the π–π overlap of their phenyl rings.

Preliminary intercalation and ion-exchange reactions of some of these layered MoPO's, like $(Me_2NH_2)_2[Mo_4O_8(PO_4)_2]$, indicate a diverse interlayer chemistry.[26]

4. Three-Dimensional (3-D) Molybdenum Phosphates. This class of MoPO's is the most diverse and has the largest number of different structure types. The class is the largest because, like the SiO_4^{4-} building blocks in the silicates, the geometry of the PO_4 tetrahedron naturally lends itself to three-dimensional structures. Although there have been at least four examples of neutral framework materials structurally characterized, most of these solids have anionic frameworks with cations occupying sites in the tunnels. This suggests that the cations are usually necessary to provide the proper size "stuffing" when the MoO_6 octahedra and PO_4 tetrahedra try to fill space, i.e., to crystallize.

The 3-D MoPO's can be divided into two broad classifications: those synthesized via high-temperature techniques ($T > 750$ °C) and those prepared hydrothermally in the range $100 \leq T \leq 400$ °C.

4.1. Three-Dimensional MoPO's Prepared at $T > 750$ °C. These high-temperature reactions must be carried out in the absence of air as Mo^{5+} is unstable with respect to Mo^{6+} under these conditions. Nearly all of the high-temperature preparations have the Mo:P ratio within a relatively narrow range, and in only a few cases is Mo:P > 1. Too much phosphate in these reactions gives rise to glasses that do not crystallize well. If too little phosphate were to be incorporated into the solid containing cationic Mo species, the framework would be less likely to carry a negative charge and therefore could not incorporate additional cations to occupy the tunnel sites (vide supra). The presence of pyrophosphate (P_2O_7) groups in these materials is common.

The syntheses are performed by simply heating appropriate amounts of an alkali-metal molybdate or MoO_3, a phosphate source (P_2O_5 or metal phosphate), and Mo metal in an evacuated quartz ampule. The reactions proceed slowly, if at all, with $T < 750$ °C but can crystallize well in the $900 < T < 1100$ °C range. The largest single crystals in these reactions often occur on the surface of the reaction mixtures. Some of the MoPO's prepared at higher temperatures are shown in Table II.

Some of the earliest work and some of the earliest structural characterization in the field of the reduced MoPO's was carried out by Kierkegaard and co-workers. In 1970 they reported the structure of $MoOPO_4$.[34] As expected from a Mo:P ratio of 1, there are equal numbers of corner-sharing MoO_6 and PO_4 polyhedra. A neutral framework reduced MoPO was also found for the compound $Mo_2P_4O_{15}$.[35]

Table II. Some 3-D Molybdenum Phosphates Prepared at High Temperature

compound	ref
1. $K_4Mo_8P_{12}O_{52}$	42
2. $TlMo_2P_3O_{12}$	43
3. $NaMoP_2O_7$	44
4. MoP_2O_7	36, 39, 41
5. $KMoP_2O_7$ and $K_{0.17}MoP_2O_7$	45
6. $RbMoP_2O_7$	46
7. $KMo_2P_3O_{13}$	46
8. $MMo_2P_3O_{12}$, M = Ca, Sr, Ba	47
9. $Na_xMoP_2O_7$	48
10. $KMo_2P_3O_{13}$	49
11. $MMo_2P_3O_{13}$, M = Ca, Sr, Ba	50
12. $NaMo_2P_3O_{13}$	51
13. $BaMo_2P_4O_{16}$	52
14. $Cs_3Mo_5P_6O_{25}$	66
15. $CsMoP_2O_7$	53
16. $Cs_2Mo_4P_6O_{26}$ and $M_4Mo_8P_{12}O_{52}$, M = Cs, Rb, K, Tl	29
17. $AgMo_5P_8O_{33}$	54
18. $CsMo_2P_3O_{13}$	55
19. $NaMo_2P_4O_{14}$	56
20. $NaMo_2P_3O_{12}$	57

The only other neutral framework in this class is MoP_2O_7,[36] **9**, which was initially identified as a powder isostructural to ZrP_2O_7. The exact structure of ZrP_2O_7 (and thus MoP_2O_7) has proved to be elusive over the years. The structure can be envisioned to be related to that of pyrite in that the P–O–P vectors in **9** lie in the same orientation and in the same space group ($Pa\bar{3}$) as the S–S groups in pyrite. In 1971 Chaunac[37] reported that under most preparative conditions ZrP_2O_7 has a weak superstructure that triples the ca. 8-Å subcell to ca. 24 Å. Unfortunately, the central O atom of the P_2O_7 group in the subcell of this structure type lies on an inversion center in the apparent space group of $Pa\bar{3}$, thus enforcing an unrealistic P–O–P angle of 180°. Later, a computer simulation of the superstructure (of the isostructural SiP_2O_7) suggested a possible structure,[38] but some of the pyrophosphate groups remained on $\bar{1}$ sites in $Pa\bar{3}$ even in the superstructure. In 1987 we solved the single-crystal structure of MoP_2O_7 in the 8-Å subcell[39] but did not report the structure, even though $R \approx 0.06$, because of the linear P–O–P angles and the chemically unrealistic Mo–O distances that gave a calculated Mo oxidation state near 6+ from bond strength–bond length calculations even though the stoichiometry was clearly Mo^{4+}. In this study it was impossible to measure a significant fraction of the superstructure reflections, with a sealed-tube X-ray source, as they were in general several orders of magnitude weaker than the reflections from the subcell. However, we recently measured hundreds of these weak superstructure reflections with the aid of synchrotron radiation at NSLS[40] and found to our surprise that even though the superstructure appears to be metrically cubic within the errors of the

(32) Corcoran, E. W., Jr. *Inorg. Chem.* **1990**, *29*, 157.
(33) Mundi, L. A.; Haushalter, R. C. In *Synthesis, Characterization and Novel Applications of Molecular Sieve Materials*; Maroni, V.; Ed.; Materials Research Society: Pittsburgh, PA, 1991.
(34) Kierkegaard, P.; Westerlund, M. *Acta. Chem. Scand.* **1964**, *18*, 2217.
(35) Minacheva, L. Kh.; Antsyshkina, A. S.; Sakharova, V. G.; Nikolaev, V. P.; Porai-Koshits, M. A. *Zh. Neorg. Khim.* **1979**; *24*, 91.
(36) Kinomura, N.; Mitsuaki, M.; Nobuhiro, K. *Mater. Res. Bull.* **1985**, *20*, 379.
(37) Chaunac, M. *Bull. Chem. Soc. Fr.* **1971**, 424.
(38) Tillmans, E.; Gebert, W.; Baur, W. H. *J. Solid State Chem.* **1973**, *7*, 69.
(39) Rheingold, A.; Haushalter, R., unpublished results.
(40) King, H. E., Jr.; Haushalter, R., unpublished results.

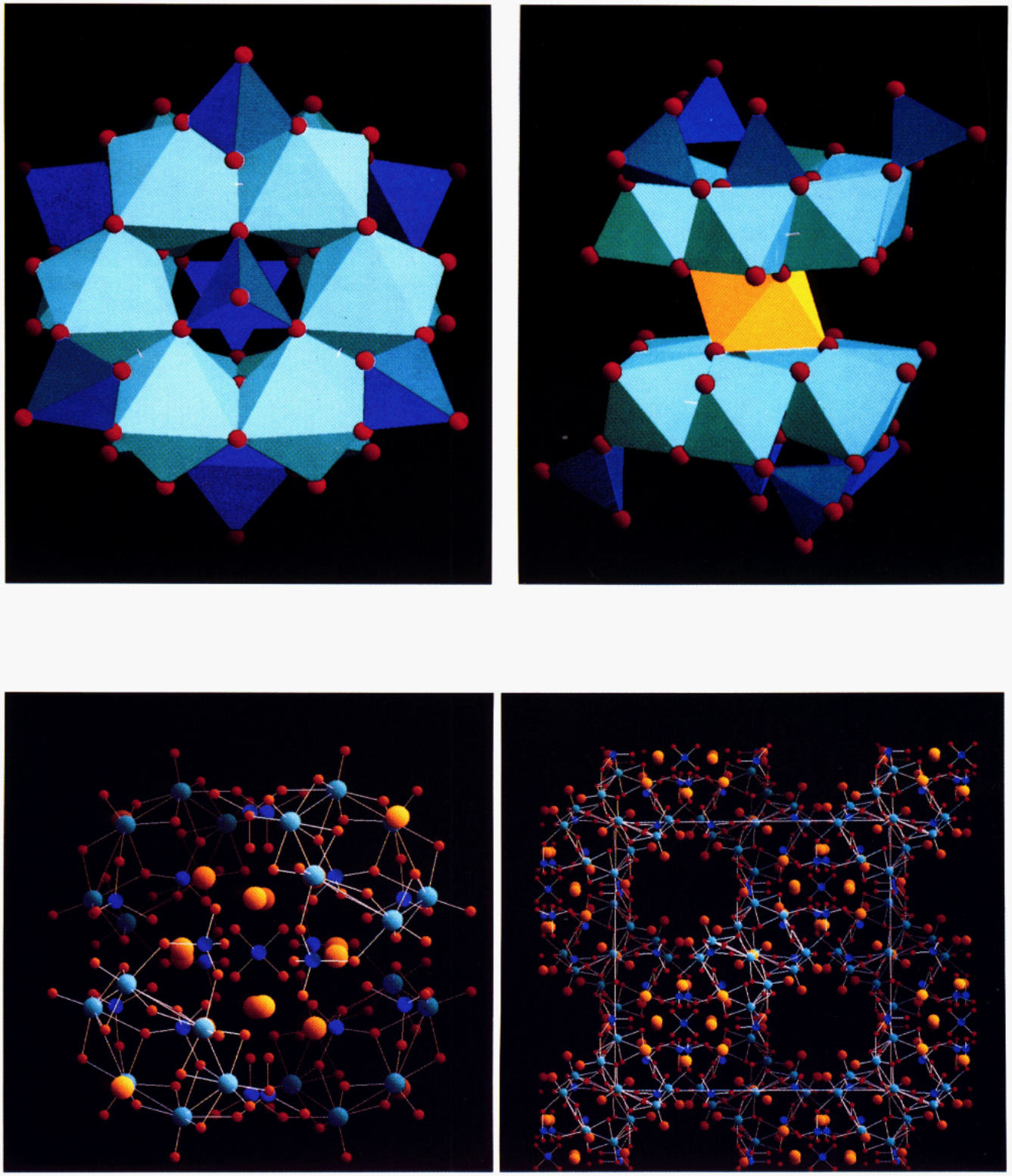

Figure 5. Top: $\{M^{n+}[Mo_6O_{15}(HPO_4)(H_2PO_4)_3]_2^{(10+n)-}\}$ cluster (**1**), composed of two $Mo_6O_{15}(HPO_4)(H_2PO_4)_3^{5-}$ units dimerized about the central M^{n+} ion and shown both in perspective and perpendicular to the pseudo-3-fold axis. Unless otherwise noted Mo = light blue, P = blue, O = red, and metal cations = yellow. **Figure 6.** Lower left: $[Na_{12}Mo_{24}O_{60}(HPO_4)_4(H_2PO_4)_{12}(H_3PO_4)]^{8-}$ clusters found in **2**. Note that the 17 polar phosphate groups are on the interior of the cluster near the 12 Na^+, and the 24 Mo=O groups are on the exterior surface. **Figure 7.** Lower right: unit cell of $(Et_4N)_6Na_{4/2}[Na_{12}(H_3PO_4)\{Mo_6O_{15}(HPO_4)(H_2PO_4)_3\}_4]\cdot xH_2O$ (**2**), with the oxygen atoms of the Mo=O groups (in orange) enlarged to emphasize how they are segregated onto the lining of the Et_4N^+ (not shown) filled tunnels.

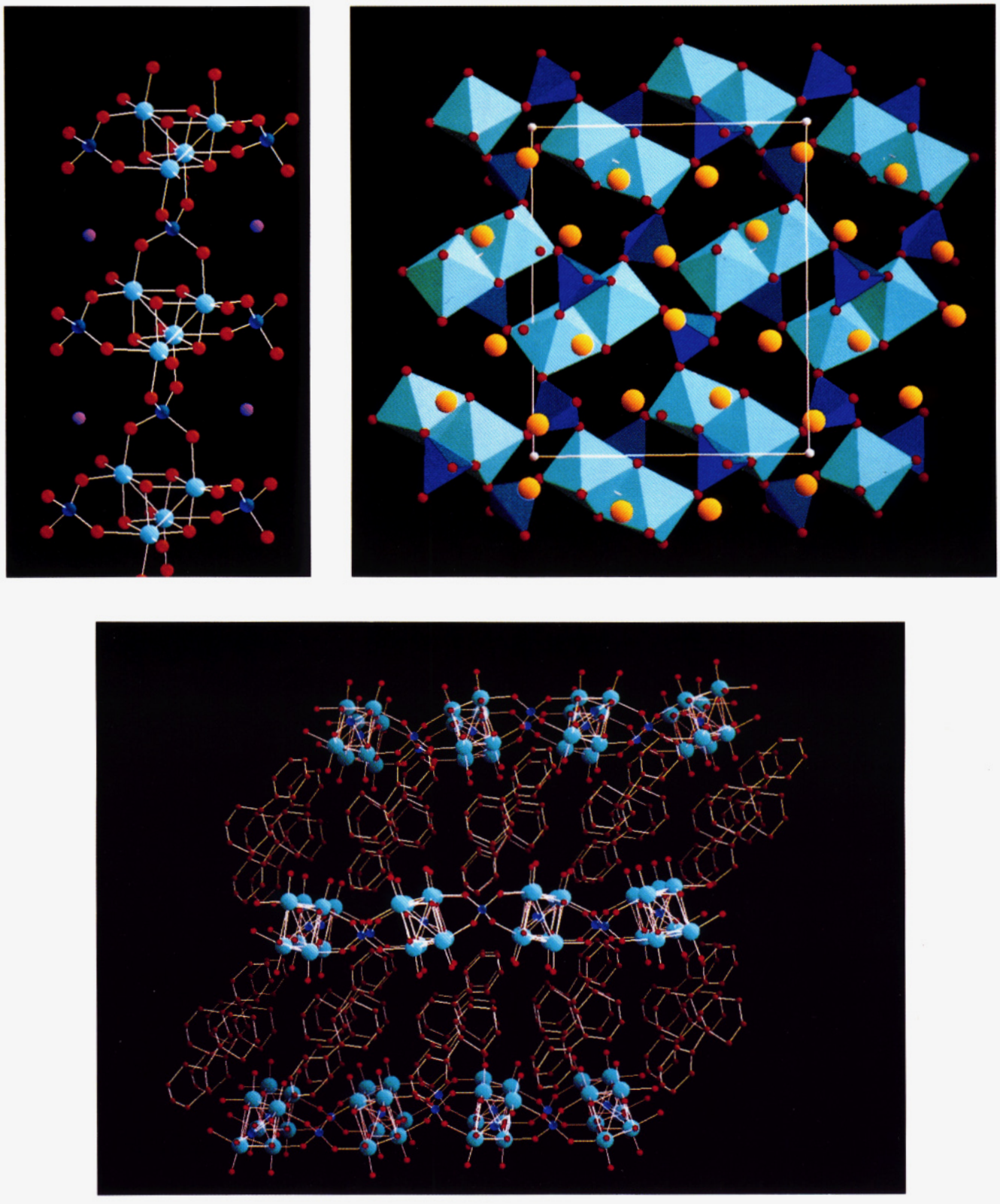

Figure 9. Upper left: view of the one-dimensional molybdenum phosphate chain, which runs along [001], found in $(Et_4N)_2[Mo_4O_8(PO_4)_{2/2}(H_{1,5}PO_4)_2]\cdot 2H_2O$ (**3**). **Figure 12.** Upper right: view of the structure of $Na_3[Mo_2O_4(HPO_4)(PO_4)]\cdot 2H_2O$ (**5**), projected onto (101) showing the connectivity of the phosphate groups to the dimolybdenum unit. The terminal P–O vectors project above and below the plane containing the layers. **Figure 14.** Bottom: view parallel to the puckered $[Mo_4O_8(PO_4)_2]^{2-}$ layers found in (4-phenylpyridine)$_2[Mo_4O_8(PO_4)_2]$ (**8**), with C and N atoms brown. Note that the organic cations pack to maximize the π–π overlap of the phenyl rings.

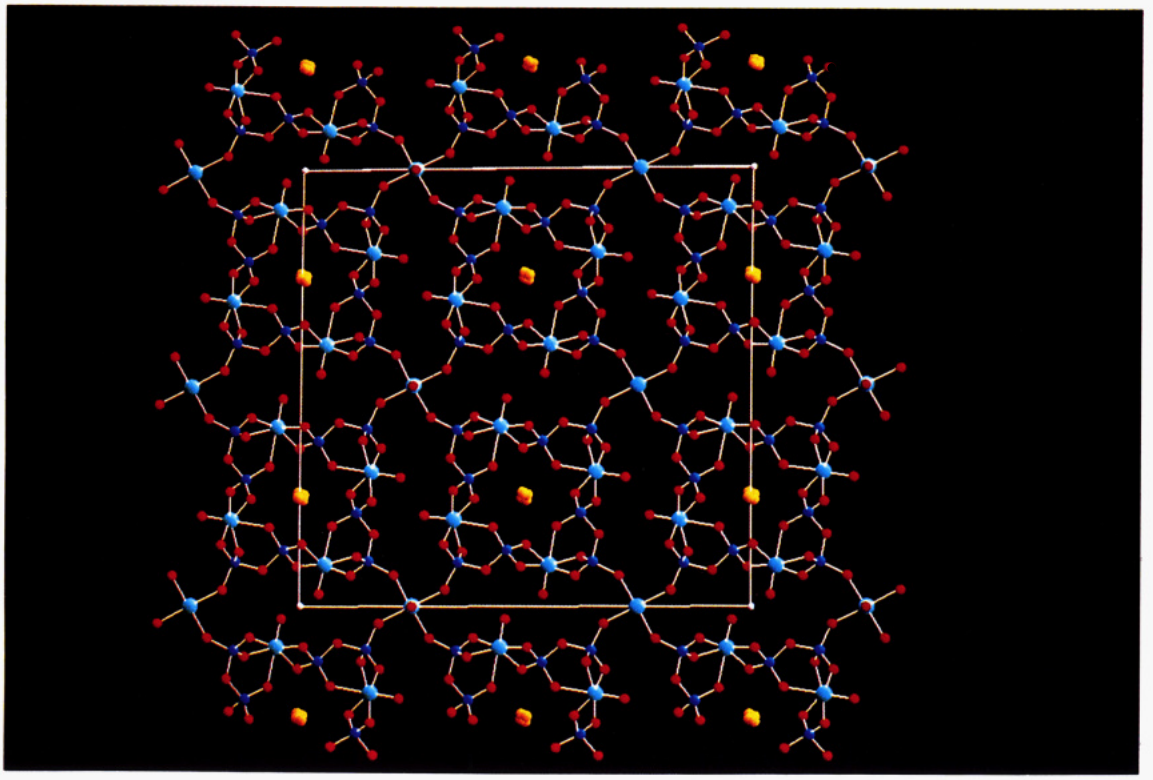

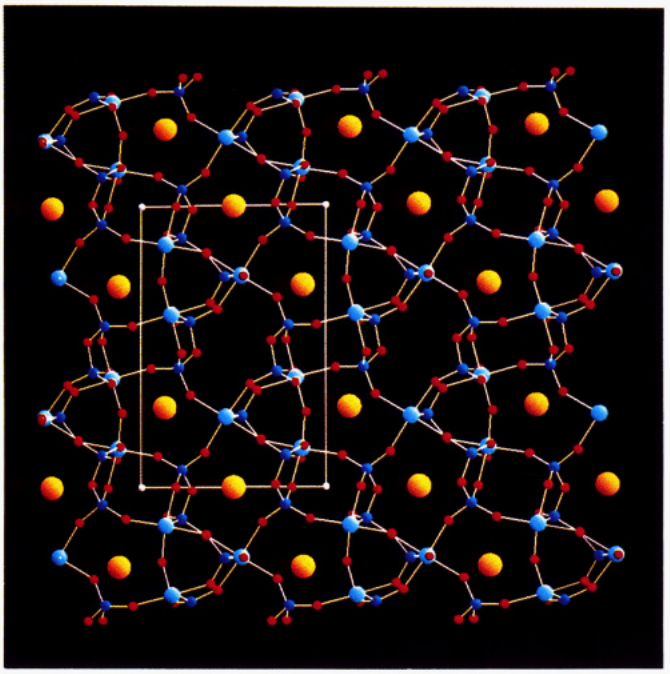

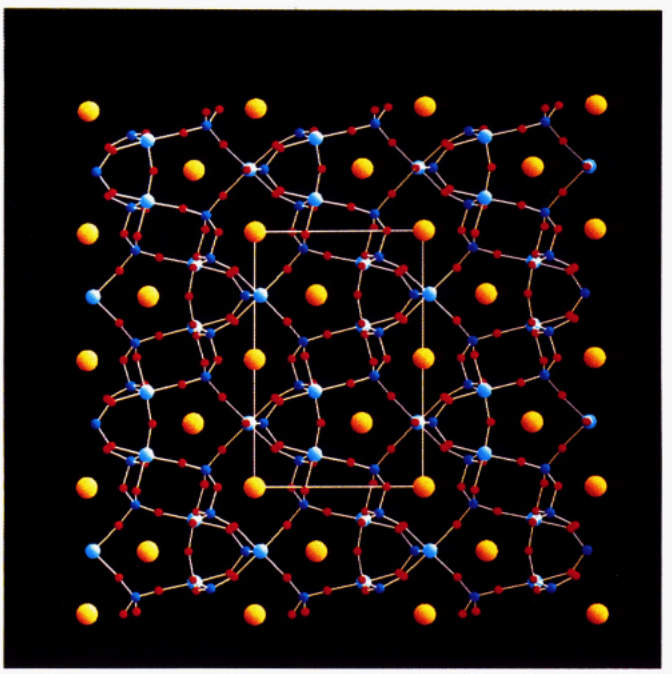

Figure 15. Top: projection of the structure of $AgMo_5P_8O_{33}$ down the short *b* axis. Note (a) the 1-D chain of disordered Ag^+ in the center of the tunnels within the large rings and (b) the 1-D chains of ···Mo═O···Mo═O··· formed the interannular corner sharing MoO_6 octahedra that also run along [001]. **Figure 16.** Bottom: representations of the structures of $Cs_3Mo_6P_{10}O_{38}$ (**10**) and $Cs_4Mo_6P_{10}O_{38}$ (11) projected down [001]. Removal of the fourth Cs^+ from 11 causes a lowering of the symmetry from monoclinic to triclinic concomitant with the disappearance of the 2_1 axis and the mirror plane.

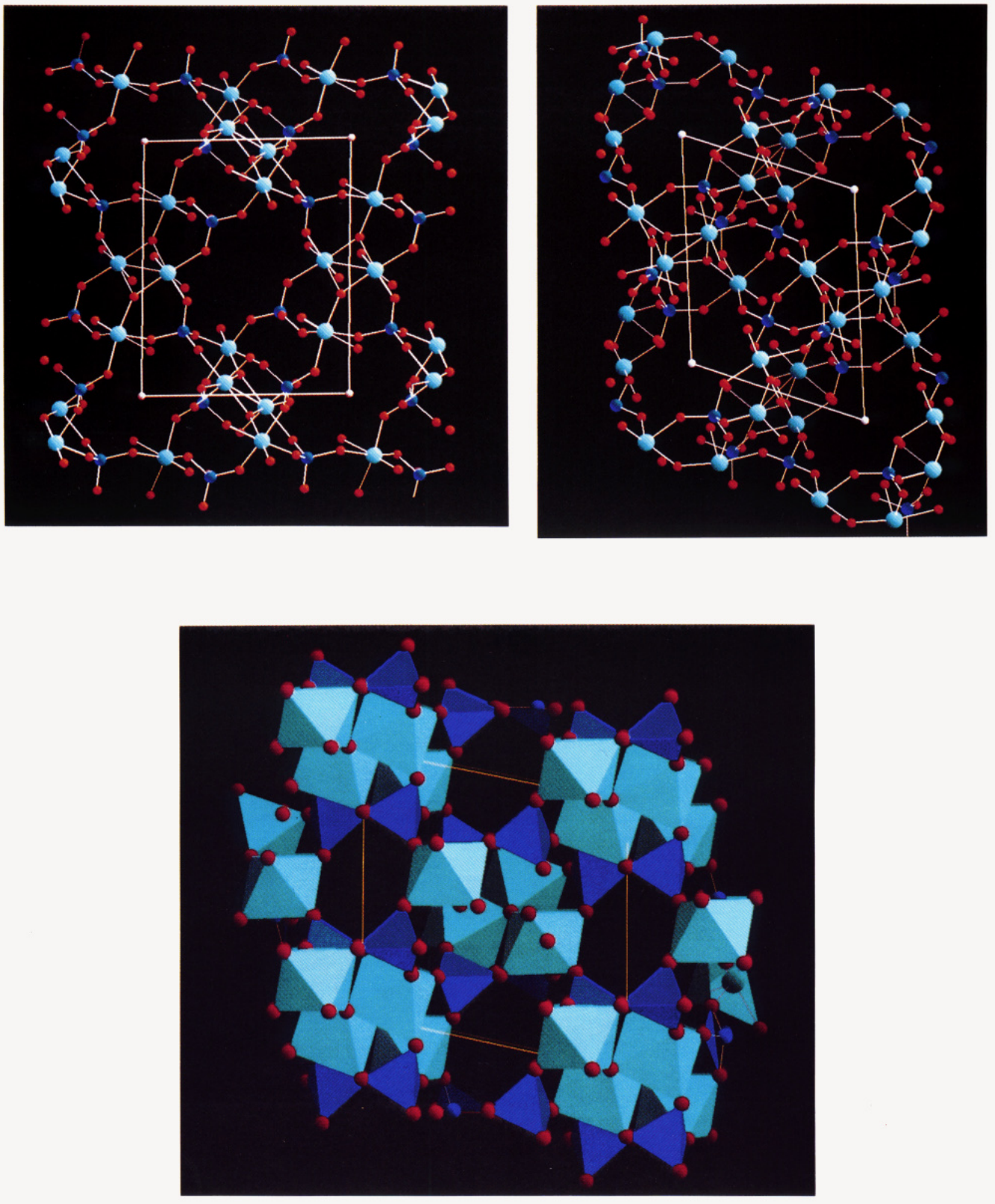

Figure 21. Top: two views of the structure of **15**, $Mo_8O_{12}(PO_4)_4(HPO_4)_2 \cdot 13H_2O$, showing how the two crystallographically independent Mo_4 units (Figure 4e) are connected to generate the open framework (upper left viewed down [001], upper right down [010]). The water molecules in the tunnels are not shown. **Figure 22.** Bottom: representation of the structure of $NH_4[Mo_2P_2O_{10}] \cdot H_2O$ **(16)** projected down [010]. The two central Mo atoms in this structure are connected by a Mo=Mo double bond at 2.453 (2) Å. The tunnels are filled in an ordered manner with H_2O and NH_4^+ (not shown).

measurements, the symmetry of the cell appeared only orthorhombic with *mmm* Laue symmetry. We still did not have enough data to solve the huge 24 × 24 × 24 Å cell. This problem with the superstructure, however, did not prevent the publication of a single-crystal structure of MoP_2O_7 recently,[41] in which no mention was made of the superstructure problem, and in which linear P–O–P bonds and an Mo oxidation state of 5.3+ (calculated from the reported Mo–O distance of 1.92 Å) were reported.

While these materials are dense framework solids, the discovery of an open-framework MoPO with alkali-metal-filled tunnels, $K_4Mo_8P_{12}O_{52}$,[42] by Leclaire and coworkers suggested that the preparation of microporous solids with octahedral–tetrahedral frameworks might be possible. Subsequently a large number of these frameworks have been discovered (Table I) that display a wealth of new structure types, bonding modes, and new crystal chemistry.

Many of the solid-state MoPO's have predominantly corner-sharing polyhedra, particularly those that are P rich and have Mo:P less than 1. For example, in $AgMo_5P_8O_{33}$[54] (Figure 15), an edge-sharing combination of $Mo^{5+}O_6$ octahedra combined with pyrophosphate groups gives rise to large rings composed of four octahedra and four pyrophosphate double tetrahedra. These rings, which are bonded together via a second type of MoO_6 unit, are filled with 1-D strings of Ag^+ disordered over several sites. Although the ionic conductivity of this material was uninvestigated, this anisotropic 1-D arrangement of partially occupied Ag^+ sites looks promising for ion conduction.

As the ratio Mo:P is increased, the MoO_6 octahedra must at some point begin the transition to further condensation: from sharing all their corners with phosphate groups to corner sharing with other MoO_6 octahedra (i.e., the formation of Mo–O–Mo bonds) to edge sharing between MoO_6 units and eventually to face sharing arrangements. One would also predict, based on the propensity of molybdenum toward metal–metal bond formation, the appearance of Mo–Mo bonds at some point. As the ratio Mo:P increases, all of the above features have been observed in MoPO's.

The beginning of corner sharing and the formation of Mo–O–Mo bonds is seen in the $Mo_6P_{10}O_{38}^{n-}$ framework and its structural relatives. Figure 4c shows a building block with $O_5Mo–O–MoO_5$ linkages containing Mo^{4+}. Figure 16a,b shows the structures of $Cs_3Mo_6P_{10}O_{38}$[58] (**10**) and $Cs_4Mo_6P_{10}O_{38}$[59] (**11**), which illustrates the effects of cation ordering on a framework geometry. Both solids have the same framework composition and differ only in amount of Cs^+. In $Cs_4Mo_6P_{10}O_{38}$, bond strength–bond length calculations clearly show that the Mo in the dimer are 4+, while the isolated Mo is 3+. In $Cs_3Mo_6P_{10}O_{38}$ the location of the odd electron is not known, but it likely resides in one of the Mo–O–Mo dimers. Note (Figure 16) that the removal of the edge-centered cation at 0, $^1/_2$, 0 in **11** causes a wholesale shifting of the atoms as the mirror plane and the 2_1 axis disappear and the symmetry of the cell drops from monoclinic to triclinic. Some of the basic structural motifs found in **10** and **11** also occur in sections of the structure of $Cs_4Mo_{10}P_{18}O_{66}$[60] with the addition of regions of composition $Mo_4P_8O_{28}$ (=$4MoP_2O_7$).

Further condensation leads to edge-sharing MoO_6 units as mentioned above in the case of $Na_3[Mo_2O_4(HPO_4)(PO_4)]·2H_2O$, which has Mo:P = 1 and a Mo–Mo single bond. Four MoO_6 units each sharing three edges with one another in the compound $Cs_3Mo_4P_3O_{16}$[61] (**12**) provides an interesting example of multiple edge sharing. This compound, which crystallizes in $P\bar{4}3m$, contains an $Mo_4O_4(PO_4)_{6/2}^{3-}$ cluster (Figure 4h) with rigorous $\bar{4}3m$ point symmetry. It has four crystallographically identical $Mo^{3.5+}$, and four μ^3-O, which together form a cube with $10e^-$ in six equivalent Mo–Mo bonds (which describe a tetrahedron) at 2.579 (5) Å. This differs from the "cubes" described above which contain two Mo^{5+}, only two Mo–Mo bonds per cube and approximate $\bar{4}2m$ point symmetry. Each cube face is capped with a PO_4 group which bridges it to an identical cube in the next unit cell. If one considers eight of these Mo_4O_4 cubes in adjacent unit cells to describe the corners of a "super cube", then the Cs^+ ions lie at the centers of the windows (i.e., each face center of the "super cube", Figure 17) circumscribed by the O atoms of the phosphate groups. The large body center of this super cube is, however, empty which is somewhat surprising for a phase prepared at 950 °C. This structure type is surprisingly diverse and has been observed previously, but without M–M bonds, in octahedral–tetrahedral combinations such as pharmocosiderite[62] ($K_{\sim 1}[Fe_4(OH)_4(AsO_4)_3]·6–8H_2O$), $K_3HGe_7O_{16}$,[63] a titanium silicate,[64] and other materials.[65] The phosphate $(NH_4)_3Mo_4P_3O_{16}$, isostructural to **12**, was prepared hydrothermally and is discussed below. Another example of the Mo_4O_4 "cube" is found in $Cs_3Mo_5P_6O_{25}$[66] (**13**), which has P_2O_7 instead of PO_4 groups, and a trigonal distortion along a cube body diagonal resulting in two sets of three Mo–Mo distances (3 × 2.558 (1) and 3 × 2.697 (1) Å). The difference in geometry between **12** and **13** had a large effect on the magnetic properties of the cluster.[66] Phosphate **12** apparently has an $S = 0$ ground state with the next excited state becoming populated at $T > 200$ K, while **13**, which also contains a magnetically active Mo^{3+} in the lattice in addition to the trigonally distorted cube,

(41) Leclaire, A.; Borel, M. M.; Grandin, A.; Raveau, B. *Eur. J. Solid State Inorg. Chem.* **1988**, *25*, 323.
(42) Leclaire, A.; Monier, J. C.; Raveau, B. *J. Solid State Chem.* **1983**, *48*, 147.
(43) Leclaire, A.; Monier, J. C.; Raveau, B. *J. Solid State Chem.* **1985**, *59*, 301.
(44) Leclaire, A.; Borel, M. M.; Grandin, A.; Raveau, B. *J. Solid State Chem.* **1988**, *76*, 131.
(45) Leclaire, A.; Borel, M. M.; Grandin, A.; Raveau, B. *J. Solid State Chem.* **1989**, *78*, 220.
(46) Riou, D.; Leclaire, A.; Grandin, A.; Raveau, B. *Sect. C: Cryst. Struct. Commun.* **1989**, *C45*, 989.
(47) Leclaire, A.; Borel, M. M.; Grandin, A.; Raveau, B. *Eur. J. Solid State Inorg. Chem.* **1989**, *26*, 45.
(48) Leclaire, A.; Borel, M. M.; Grandin, A.; Raveau, B. Z. *Kristallogr.* **1988**, *184*, 247.
(49) Leclaire, A.; Borel, M. M.; Grandin, A.; Raveau, B. *Acta Crystallogr.* **1990**, *C46*, 2009.
(50) Leclaire, A.; Borel, M. M.; Grandin, A.; Raveau, B. *J. Solid State Chem.* **1990**, *89*, 10.
(51) Costentin, G.; Borel, M. M.; Grandin, A.; Leclaire, A.; Raveau, B. *J. Solid State Chem.* **1990**, *89*, 31.
(52) Costentin, G.; Borel, M. M.; Grandin, A.; Leclaire, A.; Raveau, B. *J. Solid State Chem.* **1990**, *89*, 83.
(53) Lii, K. H.; Haushalter, R. C. *Acta Crystallogr.* **1987**, *C43*, 2036.
(54) Lii, K. H.; Goshorn, D. P.; Johnston, D. J.; Haushalter, R. C. *J. Solid State Chem.* **1987**, *71*, 131.
(55) Lii, K. H.; Wang, C. C. *J. Solid State Chem.* **1988**, *77*, 117.
(56) Lii, K. H.; Chen, J. J.; Wang, S. L. *J. Solid State Chem.* **1989**, *78*, 1.
(57) Lii, K. H.; Chen, J. J.; Wang, S. L. *J. Solid State Chem.* **1989**, *78*, 93.
(58) Lii, K. H.; Wang, C. C. *J. Solid State Chem.* **1988**, *77*, 117.
(59) Haushalter, R. C.; Lai, F. W. *J. Solid State Chem.* **1989**, *83*, 202.
(60) Haushalter, R. C.; Lai, F. W. *J. Solid State Chem.* **1988**, *76*, 218.
(61) Haushalter, R. C. *Chem. Commun.* **1987**, 1566.
(62) Zeeman, J. *Tschermaks Mineral. Petrogr. Mitt.* **1948**, *1*, 1.
(63) Zeeman, J. *Acta Crystallogr.* **1959**, *12*, 252.
(64) Reference 17 and references therein.
(65) Nowotny, H.; Wittman, A. *Monatsch. Chem.* **1954**, *85*, 558, and refs 17, 63.
(66) Lii, K. H.; O'Connor, C. J.; Haushalter, R. C. *Angew. Chem., Int. Ed. Engl.* **1987**, *26*, 549.

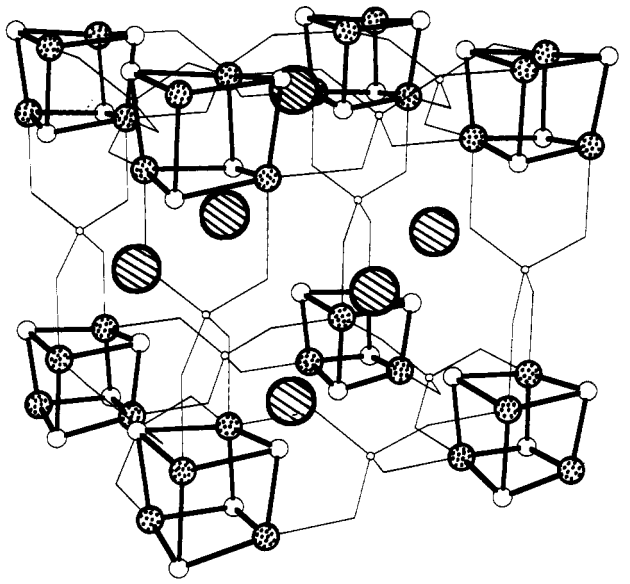

Figure 17. "Super cube" constructed from the Mo_4O_4 cubes from eight adjacent unit cells of $Cs_3Mo_4P_3O_{16}$ (**12**). Note that the Cs^+ ion positions (striped circles) correspond to the face centers of the "super cube", the P atoms (smallest white circles) are at the edge centers, and the body center of the "super cube" is empty. The radii of the phosphate O atoms have been set to zero.

displays very complicated magnetic behavior. The magnetic properties of the other "non-cube" Mo_4 units discussed below appear to be more straightforward.

It was obvious from these high-T syntheses that the octahedral–tetrahedral MoPO frameworks encompassed a large number of structure types with diverse polyhedral connectivities. But preliminary experiments indicated that the ion-exchange rates of many of these MoPO's were very slow. With the examples of the large pore mineral structures as encouragement, we began to investigate the hydrothermal syntheses of MoPO's to try to incorporate larger removable cations.

4.2. Hydrothermally Synthesized 3-D MoPD's. To access any of the internal micropore volume in the MoPO's with tunnel structures, one must empty the pores of their cationic templates or exchange them for ones smaller in size. In the MoPO's prepared at high temperatures this presented problems: the high temperature required to form the phases precludes the use of water and organic templates, and therefore one must use an inorganic cation. Even Cs^+ forms tunnels ($2d$(Cs–O) – r(O) = 2(3.2 Å) – 2.64 Å = 3.8 Å) which are probably too small to sorb even n-alkanes (diameter ca. 4.2 Å) when the cation is removed. Thus a hydrothermal approach, as in the case of the zeolites, seemed necessary.

One of the advantages of the hydrothermal synthesis of solids is that it is possible to achieve the reaction of two solid-state starting materials at much lower temperatures than those required for interdiffusion of the solids with no liquid phase present. More importantly in the present case would be the possibility of incorporating organic or hydrated inorganic (e.g., $Mg(OH_2)_6^{2+}$) cations.

To successfully prepare 3-D MoPO frameworks, one must suppress the formation of the Keggin ion-like "$Mo_{12}P$" species by keeping the Mo oxidation state at ≤5+. We have accomplished this in two ways. If the Mo source is 6+ as in MoO_3 or the alkali-metal molybdates, then Mo metal, which must be very finely divided (<2 μm), is used as the reductant. Alternatively, one can often employ the hydrolysis products of $MoCl_5$ or $MoCl_4$ as starting materials. In general, the synthesis of the MoPO's consists of reaction of the Mo source with phosphoric acid and the cationic template in water at temperatures up to ca. 400 °C. At temperatures above ca. 250 °C the use of many organic templates begins to become a problem due to thermal decomposition. In many of these preparations, the products were single phase and yielded single crystals large enough for structural characterization. We will now discuss the synthesis, structural characterization, and sorption properties of several microporous MoPO solids which have internal micropore volumes ranging from 15 to 40 vol %.

The first MoPO synthesized with a substantial micropore volume, $(Me_4N)_{1.3}(H_3O)_{0.7}[Mo_4O_8(PO_4)_2]\cdot 2H_2O$[67] (**14**), contains the same framework building block, the $Mo_4O_8(PO_4)_{4/2}^{2-}$ "cubes", found in the layered materials **6–8**. Three of the ways in which these cube building blocks can be connected together, to give the frameworks of **6–8** and **14**, are shown in Figure 18a–c. In the layered materials **6–8**, the cubes all have the same orientation with the Mo=O vectors perpendicular to the plane defined by the four surrounding phosphate groups. In **14**, the cubes are connected into a 3-D array by the up and down alteration of the planes defined by the PO_4 groups. The alteration in the orientation of these cubes causes the cell edges in **14** to double as compared to **6–8**. As shown in Figure 18b,c this orientational alteration causes "cube defects" to be present in each of the "layers" (all sections parallel to ⟨100⟩). Therefore 25% of the cubes are missing. In fact this defect ordering provides an interesting means of describing the structure. If one were to consider a 2 × 2 array

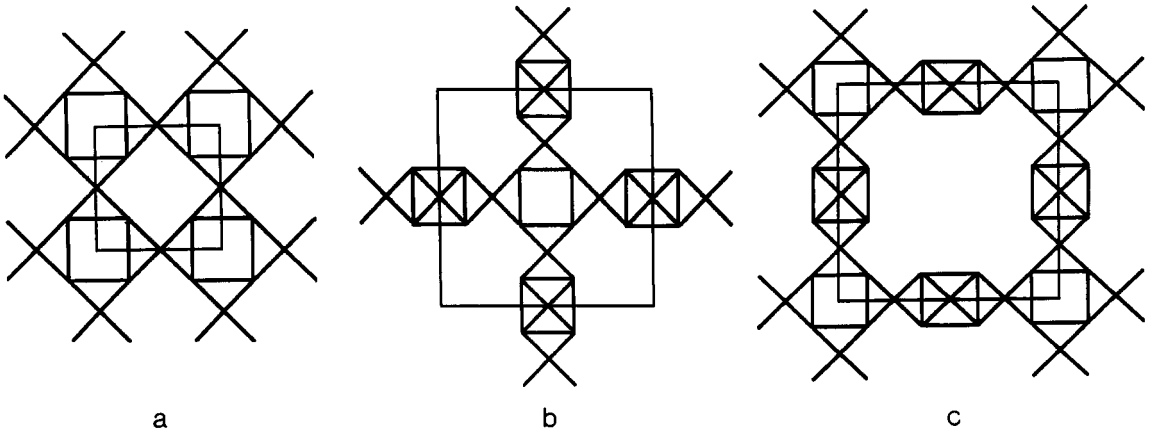

Figure 18. Schematic illustration of some possible connectivities for the $[Mo_4O_8(PO_4)_2]^{2-}$ units: (a) the planar layers as found in $Pr_4N(NH_4)[Mo_4O_8(PO_4)_2]$ and $(Et_2NH_2)_2[Mo_4O_8(PO_4)_2]$; (b) and (c) an alternative connectivity of the same units, which form every other connected "layer", in $(Me_4N)_{1.3}(H_3O)_{0.7}[Mo_4O_8(PO_4)_2]\cdot 2H_2O$ (**14**). Note how the connection of b and c together generates the large body centered cavities found in **14**. Squares are Mo_4O_4 cubes and ×'s are PO_4 groups.

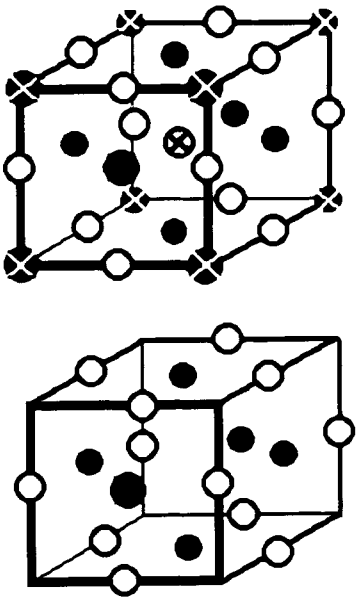

Figure 19. Schematic illustration of the vacancy ordering in NaCl vs NbO. The same relationship is found in the vacancy ordering in 14 compared to 12.

of the cubes present in the primitive cubic array in $Cs_3Mo_4P_3O_{16}$ (12), then by removing the cubes that correspond to the origin and body center in this 2 × 2 array (as well as removal of some of the phosphate groups and oxidation of the $Mo^{3.5+}$ to Mo^{5+}) one arrives at the structure of 14. It is interesting to note that the relationship of the vacancy ordering between 12 and 14 is essentially the same as that between the NbO and NaCl structure types as illustrated in Figure 19. Phosphate 14 has the molybdenyl groups from six different Mo_4O_8 cubes oriented toward the interior of the cavity, which is filled with a mixture of Me_4N^+, H_3O^+, and H_2O. The cavity containing the cations and solvent is quite large with free diameter distances between Mo=O oxygen atoms across the cavities of ca. 7-Å. The distance corresponding to the body diagonal of the cavity is even larger. However, the free diameters of the windows providing access to the cavities is only ca. 2.8 Å in diameter, thus precluding the sorption of even linear hydrocarbons. The absorption isotherms for small molecules like water show reversible behavior (Figure 20a), thus allowing one to accurately estimate the free internal volumes. Since the density of most of these MoPO frameworks is close to 3 g cm^{-3} and the density of sorbed water is near 1 g cm^{-3}, one can simply multiply the weight percent of water reversibly absorbed by 3 to obtain the approximate volume filled by the water.

In addition to the two types of cubes discussed above, two other types of Mo_4 units have been observed in the 3-D microporous MoPO's. The compound $Mo_8O_{12}(PO_4)_4(HPO_4)_2 \cdot 13H_2O$[68] (15) displays several novel structural features. It is the only MoPO that has a neutral framework and contains only water molecules as the species filling the pores. It is also the MoPO with the largest internal void volume. Phosphate 15 is prepared from MoO_3, Mo, H_3PO_4, and H_2O and is built up from two centrosymmetric, crystallographically independent Mo_4 units as shown in Figure 4e. These two tetramers are both composed of two edge-sharing MoO_6 octahedra, with Mo–Mo single bonds (2.659 (5) and 2.611 (6) Å), with the two O atoms involved in this shared edge also serving as a corner for two additional MoO_6 octahedra making these particular oxygens each three coordinate to three different Mo atoms. All five of the Mo atoms are in the 5+ oxidation state.[68] The magnetic susceptibility shows two unpaired electrons per four Mo, consistent with the two outer octahedra being

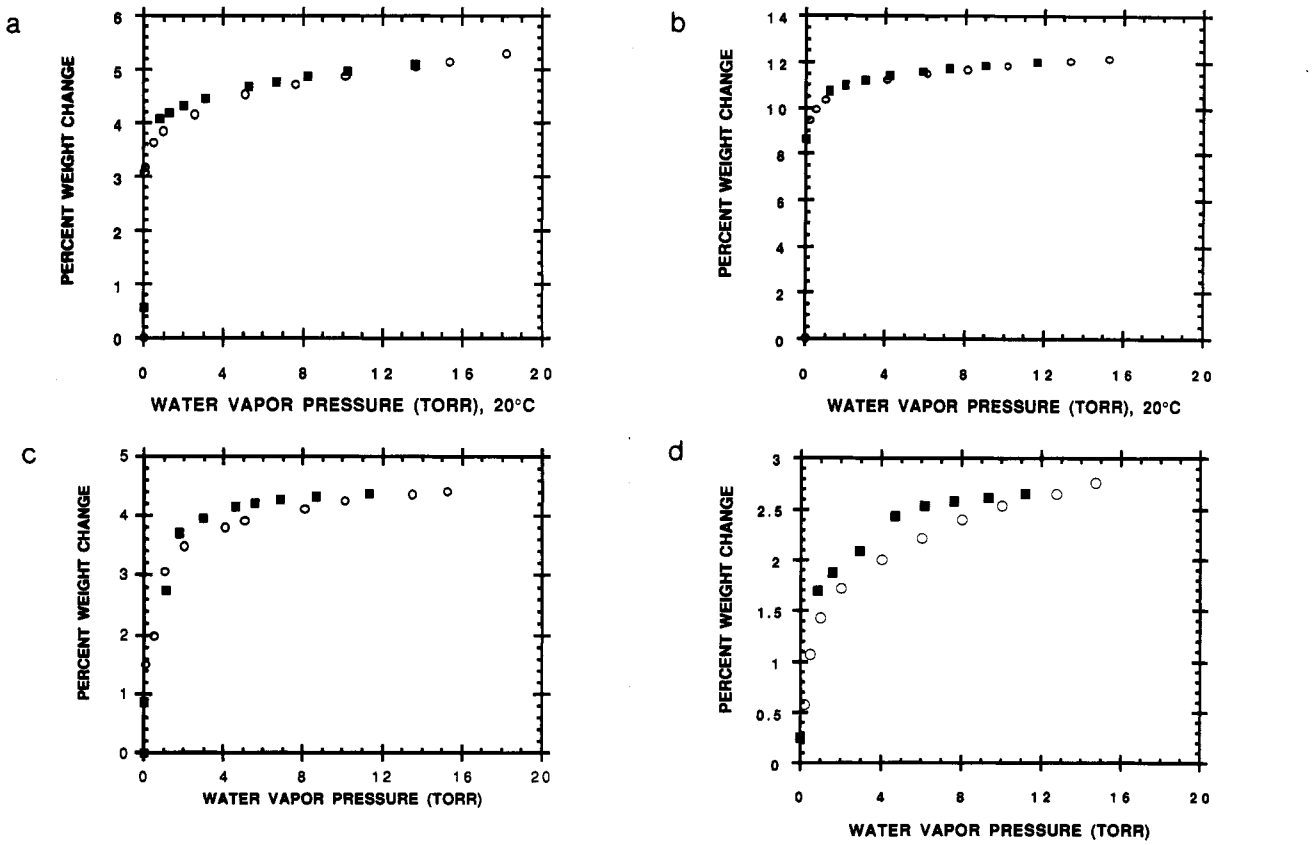

Figure 20. Water absorption isotherms obtained for several MoPO's: (a) 14, (b) 15, (c) 16, (d) 19. Isotherms a–c approximate type 1 absorption isotherms, while that of d is less perfectly reversible. The internal void volume filled in each case is obtained by multiplying the weight percent absorbed by ca. 3 (the density of the MoPO framework).

isolated d^1 Mo^{5+} and the electrons from the central Mo atoms paired in the Mo–Mo bond. As shown in the projections of the structure of **15** along the cell edge in Figure 21, the tetramers are connected into a 3-D framework in a complicated manner which generates tunnels that run along all three directions parallel to the cell edges. The water absorption isotherm for **15** (Figure 20b) shows the reversible absorption of not only the solvate water in the tunnels but the water directly ligated to Mo as well. This high degree of reversibility may be related to the high dimensionality of the pore structure. Since the powder X-ray diffraction pattern of dehydrated **15** showed it to be crystalline and the water absorption is reversible, one concludes that the majority of the Mo atoms in dehydrated **15** possess a vacant coordination site.[68] The internal void volume calculated from the sorption data is >35 vol %, which is comparable to the more open zeolite frameworks. Like **14**, phosphate **15** excludes hydrocarbons from its pores under ambient conditions.

Another 3-D MoPO built up from Mo_4 moieties is the black phosphate $NH_4[Mo_2P_2O_{10}]\cdot H_2O$[69] (**16**). This compound was prepared hydrothermally at 375 °C. The crystals of this compound were very small, and therefore the structure was determined and refined from single-crystal data collected on a 35 × 20 × 10 μm^3 crystal at beamline X10A at NSLS, Brookhaven National Laboratory. Like phosphate **15**, $Mo_8O_{12}(PO_4)_4(HPO_4)_2\cdot 13H_2O$, the tetrameric building blocks (Figure 4b) have two central MoO_6 octahedra that share a common edge, with the two O atoms involved in the shared edge serving as corners for two additional MoO_6 octahedra. Unlike the single bond connecting the two central Mo^{5+} in **15**, the two central Mo in **16** are formulated as Mo^{4+} as deduced from bond strength–bond length calculations and have a Mo=Mo double bond at 2.453 (2) Å. These tetramers condense in a complex way to form an open framework (Figure 22). The tunnels in the structure are filled with NH_4^+ and H_2O, which can be thermally removed to yield a solid that displays reversible absorption isotherms toward water (Figure 20c). The internal micropore volume is about 12 vol %. Interestingly, **16** is exactly isotypic to the naturally occurring hydrated hydroxy ferric phosphate mineral leucophosphite,[70] $K[Fe_2(PO_4)_2(OH)]\cdot 2H_2O$. In addition to the replacement of the Mo atoms in **16** by Fe, the Mo=O is replaced by Fe—OH_2, the μ^3-O is replaced by a triply bridging OH group, and the K^+ is replaced by NH_4. As expected, the molybdenum phosphate displays appreciably greater thermal stability.

While most of the hydrothermal MoPO syntheses discussed here yield a unique framework for a particular template, we have found that the 3-D $[Mo_2O_2(PO_4)_2(H_2PO_4)]^-$ framework can accommodate both organic and inorganic cations of varying size and shape. This cation variability can be understood in terms of the structures. The $[Mo_2O_2(PO_4)_2(H_2PO_4)]^-$ framework can be thought of as a derivative of the $MoOPO_4$ structure type.[34] The tetragonal $MoOPO_4$ structure contains equal numbers of corner-sharing octahedra and tetrahedra, one "layer" of which is shown in Figure 23. The O atom of the Mo=O molybdenyl group also forms the long, nearly nonbonded (ca. 2.6 Å) interaction, with the Mo in the next octahedra generating chains of –Mo–O– with alternating long and

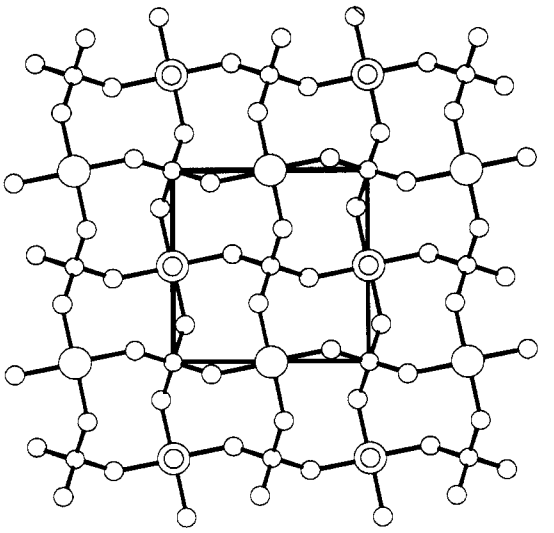

Figure 23. Projection of the structure of $MoOPO_4$ onto (001). Large circles are Mo.

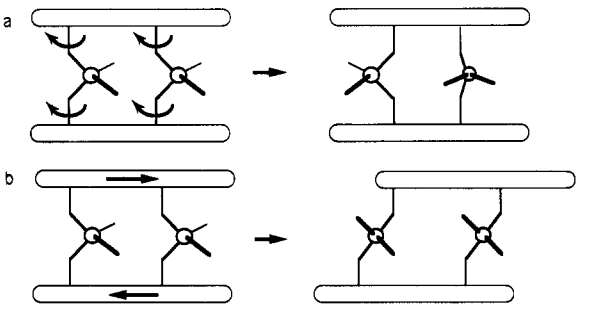

Figure 24. Schematic illustration of (a) rotation of the interlamellar phosphate groups and (b) shifting of the layers relative to one another to modify their registry.

short Mo–O distances. The $[Mo_2O_2(PO_4)_2(H_2PO_4)]^-$ structure type is related to the $MoOPO_4$ structure by replacing the –O– in the chain by HPO_4 or H_2PO_4 groups. The molybdenum environment in these materials is shown in Figure 4g. The 3-D structure consists of the $MoOPO_4$-like layers bonded together by phosphate groups. A very similar structure has been observed in $(VOSO_4)_2H_2SO_4$.[71] The cation variability is accommodated by the proper orientation of the interlamellar phosphate groups and/or the registry of the layers which is schematically illustrated in Figure 24. The framework flexibility is illustrated by the three examples **17**–**19** shown in Figure 25a–c. This is one of the most phosphorus rich of the MoPO frameworks. The most important element in the synthesis of this yellow framework seems to be the presence of excess H_3PO_4 in the reaction mixture. When the cation is H_3O^+ and/or Na^+,[72] the compound $H_3O[Mo_2O_2(PO_4)_2(H_2PO_4)]\cdot xH_2O$ (**17**) is formed, which has a body-centered tetragonal lattice with $a \approx 6.4$ and $c \approx 16$ Å. The small a dimension results from the 4-fold disorder of the interlamellar phosphate groups with the 16-Å spacing corresponding to a two-layer repeat. The compound $CH_3NH_3[Mo_2O_2(PO_4)_2(H_2PO_4)]$[73] (**18**) is C-centered monoclinic with $a \approx b \approx 9.1$ and $c \approx 8.6$ Å. The orientation of the unit cell in the $MoOPO_4$-like layers in monoclinic **18**, compared to tetragonal **17**, is rotated by 45° and expanded by $\sqrt{2}$ ($6.4 \times \sqrt{2} = 9.1$). In crystals of **17**, the interlamellar phosphate groups are all pointed in the same

(67) Haushalter, R. C.; Strohmaier, K. G.; Lai, F. W. *Science* **1989**, *246*, 1289.
(68) Mundi, L. A.; Strohmaier, K. G.; Goshorn, D. P.; Haushalter, R. C. *J. Am. Chem. Soc.* **1990**, *112*, 8182.
(69) King, Jr., H. E.; Mundi, L. A.; Strohmaier, K. G.; Haushalter, R. C. *J. Solid State Chem.* **1991**, *92*, 1.
(70) Moore, P. B. *Am. Mineral.* **1972**, *57*, 397.
(71) Tachez, M.; Theobald, F. *Acta Crystallogr.* **1981**, *B37*, 1978.
(72) Peascoe, R.; Clearfield, A. *J. Solid State Chem.*, in press.
(73) Haushalter, R. C.; Mundi, L. A.; Strohmaier, K. G. *Inorg. Chem.* **1991**, *30*, 153.

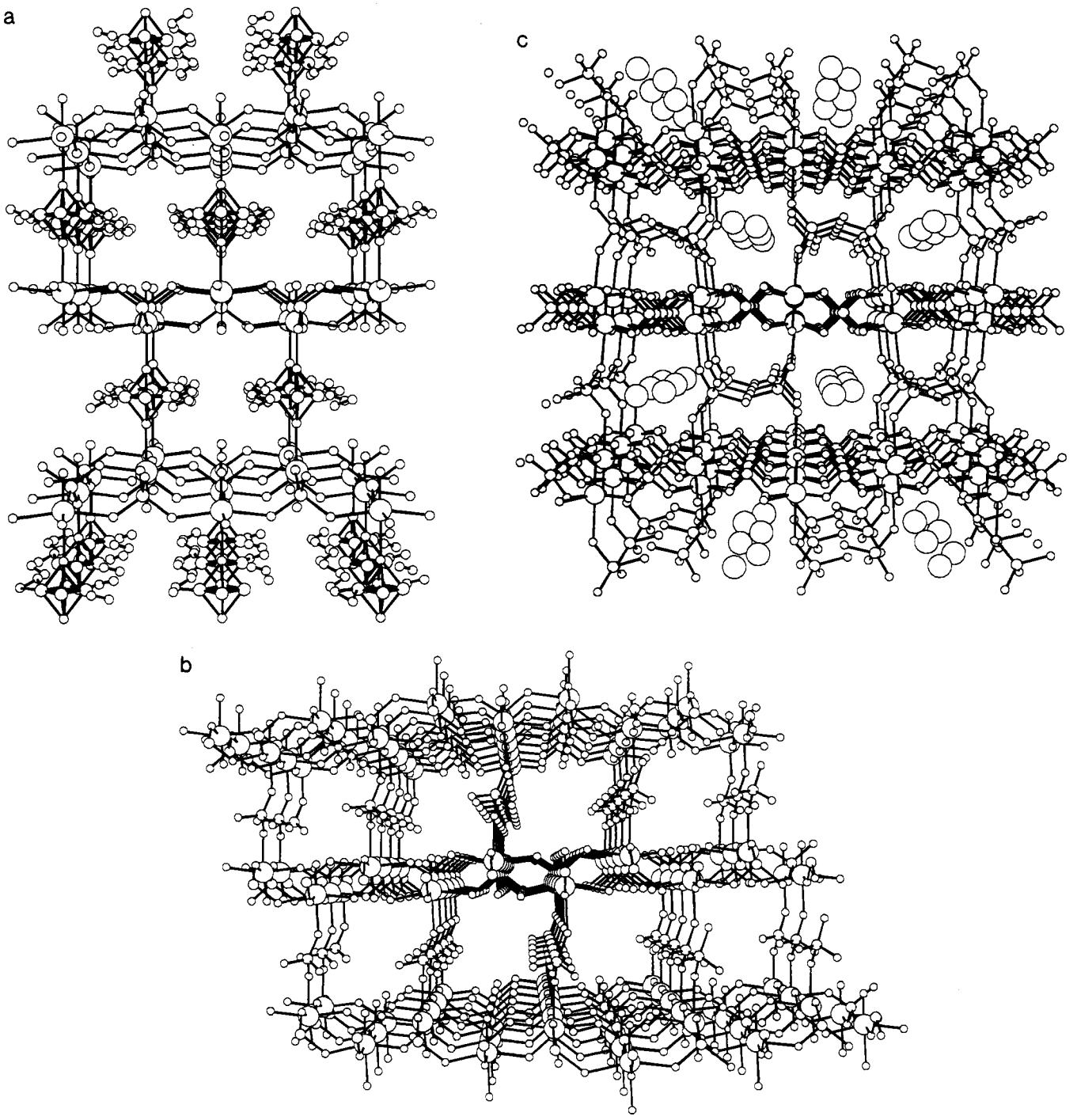

Figure 25. Structure of the three solids with the $[Mo_2O_2(PO_4)_2(H_2PO_4)]^-$ or related frameworks: (a) $H_3O[Mo_2O_2(PO_4)_2(H_2PO_4)]\cdot xH_2O$ (17); (b) $CH_3NH_3[Mo_2O_2(PO_4)_2(H_2PO_4)]$ (18); (c) $Cs(H_3O)[Mo_2O_2(PO_4)_2(HPO_4)]$ (19).

direction and therefore the space group is polar (*C*2). When the cations are Cs^+ and H_3O^+, $Cs(H_3O)[Mo_2O_2(PO_4)_2(HPO_4)]$[74] (**19**) is obtained and is monoclinic with $a \approx b \approx 9.1$ and $c \approx 16$ Å. This compound has the space between the layers divided into regions, those containing the phosphate groups and those containing the cations. As shown in Figure 26a, the interlamellar phosphate groups are combined into infinite 1-D H-bonded strings that run parallel to the $MoOPO_4$-like layers. The cations also form 1-D strings, with alternating Cs^+ and H_3O^+ cations, which run in this same direction (Figure 26b,c). Note that the number of protons on the interlamellar phosphate groups differs between **18** and **19**, which causes a change in the number of extraframework cations. Like the other 3-D MoPO's discussed above, this framework can be rendered microporous toward water. Thermal removal of the organic cation in **18** results in a solid that has approximately 30 vol % internal void space as determined from the absorption isotherms. Even the H_2O, which can be removed from the H_3O^+ cation in **19**, is reversibly sorbed and desorbed (Figure 20d).

One additional example of a microporous MoPO is found in $(NH_4)_3Mo_4P_3O_{16}$[75] (**20**), which crystallizes as black cubes that are isotypic to $Cs_3Mo_4P_3O_{16}$. This compound

(74) Mundi, L.; Yacullo, L.; Haushalter, R. *J. Solid State Chem.*, in press.

(75) Haushalter, R. C.; Mundi, L. A.; Strohmaier, K. G.; King, Jr., H. E. *J. Solid State Chem.* **1991**, *92*, 154.

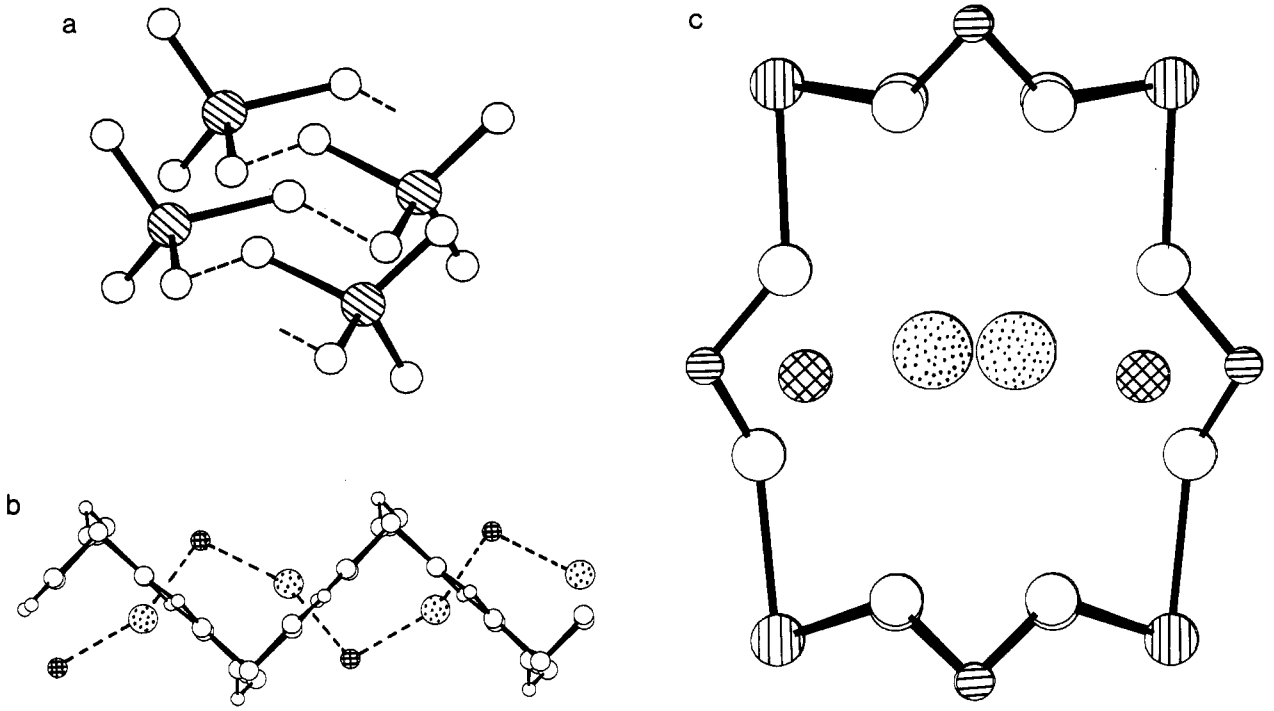

Figure 26. Illustration showing (a) the 1-D strings of H-bonded interlamellar phosphate groups with P atoms striped and two views, (b) perpendicular and (c) parallel, of the 1-D chain of altering Cs^+ (stippled) and H_3O^+ (cross-hatched).

was hydrothermally synthesized at 375 °C. Interestingly, the only two phosphates that contain Mo in an oxidation state less than <5+ are those prepared at ca. 375 °C. Neither of these phosphates, $NH_4[Mo_2P_2O_{10}]\cdot H_2O$, **16** or **20**, could be prepared, as were all of the Mo^{5+} phosphates, at 200 °C. Cubic **20** has about 12 vol % internal void space as determined from the water absorption isotherms.

4.3. Other Molybdenum Phosphates. We have recently hydrothermally prepared another very large class of new materials based on frameworks that contain molybdenum phosphate moieties connected together by transition element or main-group metal cations or groups of cations.[26] These materials have large unit cells with very complicated structures.

4. Conclusions and Future Possibilities

The main conclusion drawn from this study is that the octahedral–tetrahedral molybdenum phosphate system has a very rich crystal chemistry and contains a large number of new structure types. The MoPO's can be synthesized under a surprisingly wide variety of conditions ranging from room-temperature solutions to solid-state reactions at $T > 1200$ °C. There is no reason to think that the structural diversity displayed by the silicates and other tetrahedral frameworks cannot be matched by the octahedral–tetrahedral framework materials. It is also reasonable to assume that the formation of these solids will occur with other d-block elements besides Mo and V. A possible reason that there are more structurally characterized examples of molybdenum and vanadium phosphates than other transition element phosphates is that they crystallize so readily.

The broad goal of preparing a 3-D framework solid that is capable of sorbing molecules that could undergo shape-selective catalytic reactions at an internal d-block site has been partially realized. The problem with the solids discussed here is not that they cannot be easily prepared in high yield with a relatively defect-free pore structure but that the windows that the cavities use to communicate with the outside world are too small to allow easy passage of hydrocarbon sized molecules. In other words, it is not the incorporation of the cations into the framework that is the problem but rather their removal. It is not clear at this point exactly what synthetic conditions are required to address this problem. It could simply be that there are so relatively few known examples of microporous d-block oxides, compared to zeolites and AlPO's, that the proper synthetic conditions have not yet been discovered. The syntheses have so many variables (time, temperature, relative concentration of several reactants, nucleation and crystal growth rates, pH, starting materials, etc.) that it is still difficult to navigate through the large parameter space. Another possibility is that the interior surfaces of the MoPO type solids are too polar to easily incorporate larger organic cations (most of the ammonium cations incorporated thus far have relatively small alkyl groups).

A more complete understanding of the factors influencing the synthesis and properties of microporous d-block metal oxides will have to await the preparation of additional examples. The solids discussed here, as well as the transition metal–molybdenum phosphate frameworks recently prepared by us,[26] suggest that many more examples will be forthcoming.

Acknowledgment. We are grateful to the staff of the Molecular Structure Corp., particularly Dr. Bev Vincent, for solving many of the X-ray structures discussed here. We also thank our coauthors listed in the publications, especially K.-H. Lii, F. Lai, H. King, J. Johnson, P. Moore, H. G. von Schnering, and J. Zeeman for their important contributions and insight.